RESEARCH ARTICLE

A telomerase with novel non-canonical roles: TERT controls cellular aggregation and tissue size in *Dictyostelium*

Nasna Nassir[1], Geoffrey J. Hyde[2], Ramamurthy Baskar[1]*

1 Department of Biotechnology, Bhupat and Jyoti Mehta School of Biosciences, Indian Institute of Technology-Madras, Chennai, India, **2** Independent Researcher, Randwick, New South Wales, Australia

* rbaskar@iitm.ac.in
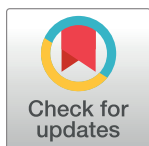
Abstract

Telomerase, particularly its main subunit, the reverse transcriptase, TERT, prevents DNA erosion during eukaryotic chromosomal replication, but also has poorly understood non-canonical functions. Here, in the model social amoeba *Dictyostelium discoideum*, we show that the protein encoded by *tert* has telomerase-like motifs, and regulates, non-canonically, important developmental processes. Expression levels of wild-type (WT) *tert* were biphasic, peaking at 8 and 12 h post-starvation, aligning with developmental events, such as the initiation of streaming (~7 h) and mound formation (~10 h). In *tert* KO mutants, however, aggregation was delayed until 16 h. Large, irregular streams formed, then broke up, forming small mounds. The mound-size defect was not induced when a KO mutant of *countin* (a master size-regulating gene) was treated with TERT inhibitors, but anti-countin antibodies did rescue size in the *tert* KO. Although, conditioned medium (CM) from *countin* mutants failed to rescue size in the *tert* KO, *tert* KO CM rescued the *countin* KO phenotype. These and additional observations indicate that TERT acts upstream of *smlA/countin*: (i) the observed expression levels of *smlA* and *countin*, being respectively lower and higher (than WT) in the *tert* KO; (ii) the levels of known size-regulation intermediates, glucose (low) and adenosine (high), in the *tert* mutant, and the size defect's rescue by supplemented glucose or the adenosine-antagonist, caffeine; (iii) the induction of the size defect in the WT by *tert* KO CM and TERT inhibitors. The *tert* KO's other defects (delayed aggregation, irregular streaming) were associated with changes to cAMP-regulated processes (e.g. chemotaxis, cAMP pulsing) and their regulatory factors (e.g. cAMP; *acaA*, *carA* expression). Overexpression of WT *tert* in the *tert* KO rescued these defects (and size), and restored a single cAMP signaling centre. Our results indicate that TERT acts in novel, non-canonical and upstream ways, regulating key developmental events in *Dictyostelium*.

Author summary

When cells divide, their chromosomes are prone to shrinkage. This risk is reduced by an enzyme that repairs protective caps on each chromosome after cell division. This enzyme,

telomerase, also has several other important but unrelated roles in human health. Most importantly, via one or other of its functions, both high and low levels of the enzyme can contribute to cancer. We have studied, for the first time, the roles played by telomerase in the life-cycle of the cellular slime mould, *Dictyostelium discoideum*, a model system with a rich history of helping us understand human biology. While we did not find any evidence of telomerase having the features typically needed to repair a chromosome, telomerase was necessary for many aspects of development. The *Dictyostelium* telomerase mutant we generated shows delayed aggregation and forms irregular fruiting bodies. The *tert* mutant miscalculates, in effect, how big those fruiting bodies should be, and they end up being too small. These results are significant because they show, for the first time, that a telomerase can influence tissue size regulation, a process central to a wide range of cancers.

Introduction

Each time a chromosome replicates, it loses some DNA from each of its ends. This is not necessarily problematic, because the chromosome is initially capped at each end by a sacrificial strand of non-coding DNA, a telomere [1–3]. Further instances of replication, however, can expose the coding DNA, unless the cell can keep repairing the shortened telomeres, by the action of the enzyme complex, telomerase. Accordingly, telomerase, whose main subunits comprise a reverse transcriptase (TERT), and the telomerase RNA component (TERC) [4], has much significance in the biology and pathology of multicellular organisms. As somatic tissues age, for example, telomerase is downregulated, and the resulting telomeric dysfunction can lead to chromosomal instability and various pathologies, including disrupted pregnancies and cancer [5–7]. In other cases, the upregulation of telomerase is also associated with, and a biomarker of, some cancers, because it allows the unchecked proliferation of immortalised tumour cells [6, 8]. Telomerase also has many non-canonical roles, in which telomere maintenance, or even telomerase activity, is not required [9, 10]. For example, telomerase is known to have non-canonical roles in neuronal differentiation [11], RNA silencing [12], enhanced mitochondrial function [13], cell adhesion and migration [14, 15] and various cancers [9, 16].

Our understanding of telomeres and telomerase began, and has continued to develop, through the study of model organisms such as *Drosophila*, *Zea mays*, *Tetrahymena*, yeast and mice [2, 3, 17–21]. One model system in which the possible roles of telomerase have not yet been addressed is *Dictyostelium discoideum*. This system has proved its usefulness in many contexts, including the study of human diseases [22–26]. One of its advantages is that the processes of cell division (i.e. growth) and development are uncoupled [27], making the organism a highly tractable system for the study, in particular, of differentiation and tissue size regulation [28–35]. In culture, when its bacterial food source is abundant, *D. discoideum* multiplies as single-celled amoebae. This leads to denser colonies, and exhaustion of the food supply. The rising concentration of a secreted glycoprotein, CMF, triggers the organism to switch to a multicellular mode of development [34, 36]. With no resources for further cell proliferation, the amoebae move, in a radial pattern of streams, towards centres of aggregation. Rising levels of secreted proteins, of the counting factor (CF) complex [37, 38], trigger a series of changes that lead to breaking up of the streams, which therefore no longer contribute cells to the original aggregate. Each aggregate, which will typically contain 20, 000 to 100,000 cells [39], now rounds up into a mound, which then proceeds through several life-cycle stages, finally forming a spore-dispersing fruiting body about 1-2mm high [34, 40]. Mounds can also develop from the breaking-up of a large stream (or aggregate), a process similarly regulated by CF [29, 41].

The generic term, 'group', can be used to address the fact that mounds develop from clusters that arise in these slightly different ways, but in this paper we will refer to 'mounds'. Some of the processes and regulators involved in our very abbreviated account of the life-cycle are shown in Fig 1, which focuses on those elements examined in this study.

In addition to being uncoupled from growth, development in *D. discoideum* has other features that make it potentially useful as a model system for the understanding of telomerase-based pathologies, in particular cancers that arise from disruption of non-canonical functions. First, as indicated in Fig 1, development in *D. discoideum* depends on properly regulated cell motility and cell adhesion, two processes fundamental to metastasis. Second, the switch to multicellular development, and the control of aggregate, mound and hence fruiting body size are influenced by various secreted factors that, respectively, promote aggregation and regulate
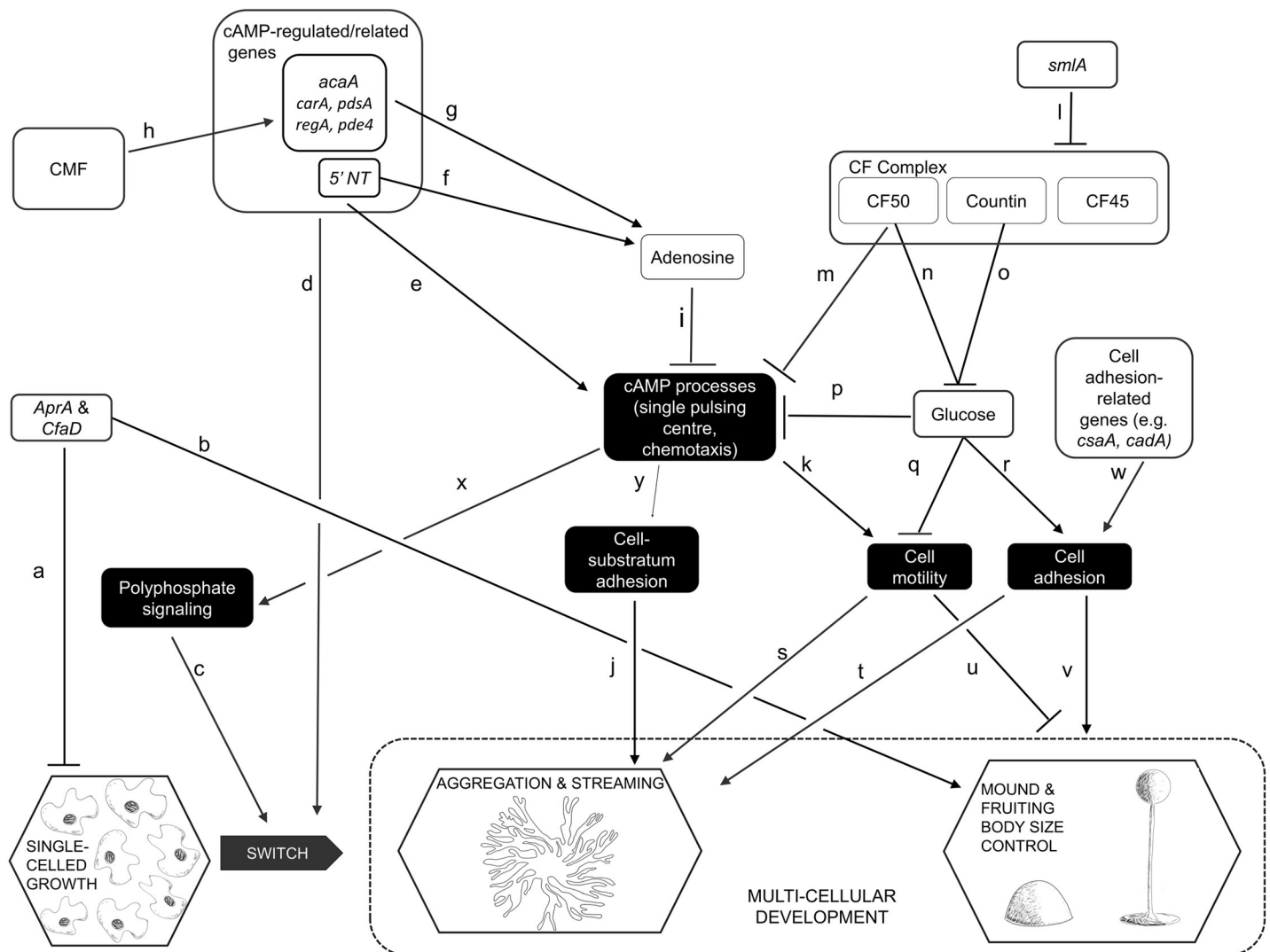
Fig 1. Some of the events, processes and regulators of growth and development in *D. discoideum*. This figure depicts only a small number of the hypothesized regulatory pathways of *Dictyostelium* growth and development, focusing on those that were examined experimentally in this study. A line ending in an arrowhead suggests that the first element directly or indirectly promotes the activity or levels of the second; inhibition is suggested by a line ending in a cross-bar. Published works that report on the nature of each pathway within the network are as follows: a[31], [42]; b[31]; c[43]; d[44], [45], [46]; e[47], [48], [49], [50]; f[51]; g [52], [53]; h[54–56]; i [57], [35]; j[58]; k[59], [60], [61]; l[28], [41]; m[29]; n[37]; o[62], [63]; p[64]; q[64], [65]; r[64]; s[66]; t[65]; u[67]; v[68], [41]; w[69], [70]; x[43]; y[71].

tissue size, in ways analogous to the regulation of tumour size by chalones [42, 72]. Third, a putative TERT has been annotated in the *D. discoideum* genome. It is not known if the RNA component of telomerase (TERC) is present [73] and, in any case, extrachromosomal rDNA elements at the ends of each chromosome in *D. discoideum* suggest a novel telomere structure [74]. Thus, telomerase in this organism may have a separate mechanism for telomere addition or might have non-canonical roles. As yet, however, there have been no functional studies of TERT reported for *D. discoideum*.

In this study, we characterize the gene *tert* in *D. discoideum*, showing that it has both RT and RNA binding domains. We describe the pattern of *tert*'s expression levels during all stages of development, assay for any canonical telomerase function, and examine the effects of knocking out the gene's function on development. The *tert* mutant exhibits a wide range of developmental defects, suggesting that wild-type TERT targets multiple elements of the regulatory network depicted in Fig 1. Most interestingly, these defects, and the results of experiments by which we attempt to rescue, or phenocopy, the *tert* KO phenotype, suggest that this telomerase influences the activity of *smlA*, and processes downstream of it. *Tert* thus emerges as one of the upstream genes of the cell-counting pathway, and its overall influence indicates that, despite having no obvious canonical activity, a telomerase can nevertheless play major regulatory roles by virtue of its non-canonical targets.

Results and discussion

D. discoideum expresses *tert*, a gene encoding a protein with telomerase motifs

Extending previous predictions of *tert* encoding a protein with telomerase motifs [75], our use of the Simple Modular Architecture Research Tool (http://SMART.embl-heidelberg.de) and UniProt (Q54B44) revealed the presence of a highly conserved reverse transcriptase domain and a telomerase RNA binding domain (S1 Fig). These are characteristic of a telomerase reverse transcriptase [76], supporting the idea that the gene we characterized indeed encodes for TERT. The *Dictyostelium* TERT protein shares 23% and 18.7% identity with human and yeast TERT protein respectively (Pairwise sequence Alignment-Emboss Needle). The protein sequence identities between the TERT of *D. discoideum* and five other species are tabulated in S1 Table. In the case of the identity with the TERT of humans, the strongest homologies are seen in the reverse transcriptase domain. We did a phylogenetic analysis to examine the relatedness of DdTERT with that of other organisms. For this, TERT amino acid sequences from different organisms were obtained from the NCBI database or Dictybase (http://www.dictybase.org/) or SACGB database (http://sacgb.leibniz-fli.de) and compared with TERT of *D. discoideum*. Multiple sequence alignment of the TERT amino acid sequences of various organisms including other social amoebae were used to create the phylogenetic tree, employing the MUSCLE alignment feature of MEGAX software [77]. The phylogenetic analysis suggests that *D. discoideum* TERT falls in a separate clade and is likely to be a distant relative of vertebrate homologs (S2 Fig). The evolutionary history was inferred using the Neighbor-Joining method [78]. The evolutionary distances were computed using the p-distance method and the units shown are the number of amino acid differences per site.

Further, using the fold recognition technique on the I-TASSER server, the structure of *D. discoideum* TERT was predicted using *Tribolium castaneum* (telomerase in complex with the highly specific inhibitor BIBR1532; PDB-5cqgA) as a template (S3 Fig). The modeled structure of *Dictyostelium* TERT also suggests that *D. discoideum* has a structurally conserved TERT (S3 Fig).

Telomerase activity, if any, can be ascertained by performing a Telomeric Repeat Amplification Protocol (TRAP) assay, and activity has been successfully detected in organisms such as humans, *C. elegans*, yeast, *Daphnia*, and plants [79–84]. However, while human cell lines (HeLa, HEK) did show telomerase activity, we did not detect any telomerase activity in *D. discoideum* cell extracts (S4 Fig). This concurs with previous findings, namely that the telomeres of *D. discoideum* have a novel structure [85], and that, in other organisms, TERT has several non-canonical roles [11–13].

Constitutive expression of telomerase during growth and development in *D. discoideum*

In humans, telomerase expression is reported to be low in somatic cells compared to germline and tumour cells [86]. To ascertain if *tert* expression is differentially regulated during growth and/or development, we performed qRT-PCR using RNA from different developmental stages (0, 4, 8, 10, 12, 16 and 24 h after starvation). *Tert* expression is higher in development than during growth, (8h and 12 h) (Fig 2), implying that *tert* plays a prominent role beyond the point at which *D. discoideum* is responding to starvation. Expression also shows a marked biphasic pattern, with the first peak at 8h (when streams are forming), a big dip during stream breaking (10h) and then rising gradually again to peak at about the time of mound formation (12h).

tert KO leads to delayed development, irregular streaming, and smaller mounds and fruiting bodies

To understand the possible non-canonical roles of *tert* in development of *D. discoideum*, *tert* KO cells generated by homologous recombination were seeded at a density of $5x10^5$ cells/cm^2 on non-nutrient buffered agar plates and monitored throughout development. While aggregates appeared by 8 h in the wild-type, and streams began to break at 10 h, in the mutants there was a further 8 h delay before aggregates were seen, and stream breaking began at about 18 h. Because of these delays, 'during aggregation', in this study, refers to 8 h in WT and 16 h in the *tert* KO, and 'during stream breakup' refers to 10 h in WT and 18 h in the *tert* KO.
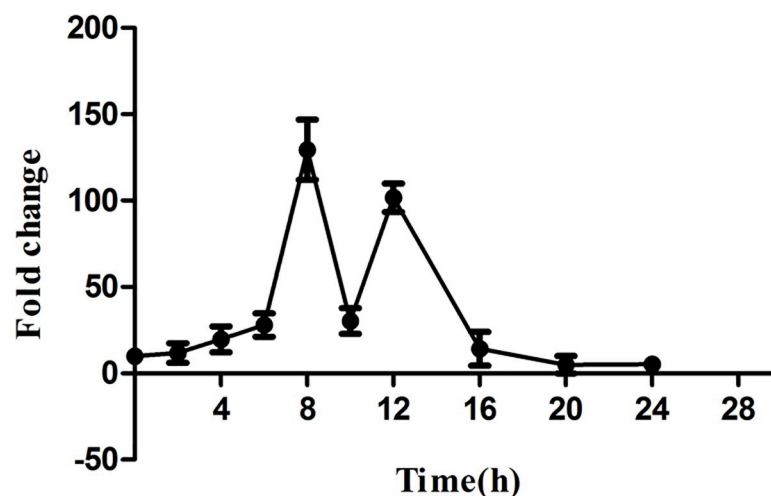
Fig 2. *Tert* expression during growth and development in *D. discoideum*. *Tert* is a single copy gene in *Dictyostelium*. Total RNA was extracted from *Dictyostelium* strain AX2 during vegetative growth and development. To analyze *tert* expression, qRT-PCR was carried out and the fold change was calculated. *rnlA* was used as a control. Time points are shown in hours (bottom). Error bars represent the mean and SEM (n = 3).

Wild-type cells formed long streams of polarized, elongated cells leading to aggregation, but *tert* KO cells did not form well-defined streams, failing to aggregate even at 5×10^4 cells/cm^2 (wild-type cells aggregated even at a density of 2×10^4 cells/cm^2), suggesting an inability to respond to aggregation-triggering conditions (S5 Fig). The mutant's streams were also larger (Fig 3A). In contrast to streams moving continuously towards the aggregation centre in WT, *tert* KO streams break while they aggregate (S1 and S2 Videos). They did eventually form aggregates, largely by clumping. During the early stages of aggregate formation, the number of aggregation centres formed by the *tert* KO was only 10% of that formed by WT (Fig 3B, p<0.0001). Due to uneven fragmentation, the late aggregates were also of mixed sizes. The *tert* KO cells did eventually form all of the typical developmental structures, but by the mound stage, continued fragmentation had resulted in the mounds being more numerous, and smaller, on average, than in the WT. This was also the case for fruiting bodies.

Thus, with reference to Fig 1, *tert* appears to play roles in multiple aspects of *Dictyostelium* development: the timing of aggregation; streaming; and the regulation of the size of the mound and fruiting body (Table 1A and 1B).

Many processes and regulators are potentially involved in the phenotypic changes of the *tert* KO

Given the wide-ranging phenotypic defects seen in the *tert* KO, it seemed likely that *tert* is one of the key regulators of development in *D. discoideum*, affecting many of the processes and regulators depicted in Fig 1. We thus monitored the activity or levels of a number of those elements, comparing the wild-type and *tert* KO (summarised in Table 1A and 1B). As that summary shows, the *tert* KO showed significant changes from the wild-type in three broad areas: components of the mound-size regulation pathway; cAMP-related processes/regulators; and adhesion-related processes/regulators. As is clear from Fig 1, the factors that influence these features overlap considerably, both in terms of interacting with each other, and in regulating more than one of the various developmental stages disrupted in the *tert* KO.
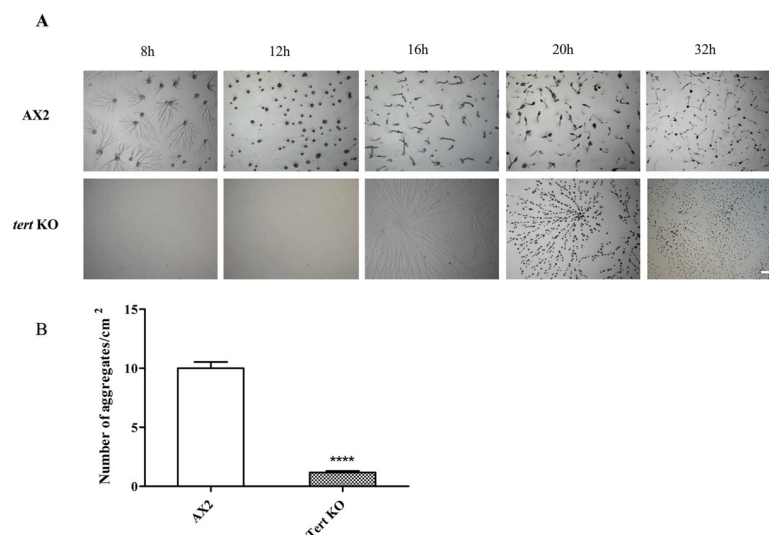
Fig 3. Developmental phenotype of *tert* KO. (A) AX2 and *tert* KO cells plated on 1% non-nutrient KK$_2$ agar plates at a density of 5×10^5 cells/cm^2 were incubated in a dark, moist chamber. After 16 hours, large aggregate streams were formed in *tert* KO. The time points in hours are shown at the top. Scale bar:0.5 mm; (n = 3). (B) Quantitative measurement of aggregation. The number of aggregation centres was counted per centimetre square area. Level of significance is indicated as *p<0.05, **p<0.01, ***p<0.001, and ****p<0.0001; (n = 3).

Table 1. Phenotypic differences between wild-type and *tert* KO development of *D. discoideum*, and some possible causal factors.

	Timing of delay to aggregation	Streaming and aggregation	Mound (and fruiting body) size	Mound-size regulation pathway		
				smlA expression levels	*Countin* expression levels	Glucose levels
tert KO cells	Delayed (by 8h)	Fragmented, uneven aggregates	Small	Low	High*	Low*

	cAMP-related factors (streaming & delay regulation)					Adhesion-related factors (streaming and mound-size regulation)			Delay-specific regulation
	Levels of cAMP-related genes: *acaA, carA, 5'NT, pdsA, regA, pde4*	Adenosine/ 5'NT Levels	cAMP centres	cAMP levels	cAMP-based chemotaxis	*csaA, cadA* expression levels	Cell-cell adhesion	Cell-substratum adhesion	Poly-phosphate levels
tert KO cells	Low at 4h-10h; High by 12h	High/high during stream break; low after. *	Many*	Low*	Abnormal	Low	Low	Low	Low

*An asterisk indicates an atypical process (or level) in the *tert* KO cells for which a rescue attempt was made (see Table 2).

https://doi.org/10.1371/journal.pgen.1008188.t001

Nevertheless, we think it is useful to consider each of them in turn. As we do so below, we describe a series of experiments that largely fall into two broad categories, as shown in summary form in Tables 2 and 3: Those that attempt to rescue the normal phenotype in *tert* KO cells (Table 2); and those that attempt to phenocopy, or induce, the *tert* KO phenotype in wild-type cells (Table 3). First, however, we describe some experiments that support the direct involvement of *tert* in the effects already noted.

Support for the involvement of *tert* itself in the *tert* KO

To support the idea that the changes observed in the *tert* KO are, in the first instance, due to changes involving *tert* itself, and not some other factor, we took two approaches: Overexpression of *tert*, and the use of TERT inhibitors. Most importantly, overexpression of wild-type TERT (act15/gfp::*tert*) in *tert* KO cells rescued all three of the phenotypic defects (Fig 4A, S3 Video; Table 2), suggesting that the *tert* KO phenotype is not due to any other mutation. Next,

Table 2. Attempts to rescue normal phenotype (or aggravate the KO phenotype) in *D. discoideum tert* KO cells.

	Timing of delay to aggregation	Streaming and aggregation	Mound and fruiting body size
Overexpression of WT *tert*	Rescue	Rescue	Rescue
Overexpression of human *tert*	No Rescue	No Rescue	No Rescue
WT cells (10–50% of total cells)	Full rescue at 50%	No Rescue	No Rescue
WT Conditioned Medium	No Rescue	No Rescue	No Rescue
Anti-countin or anti-CF50 antibodies	No Rescue	Part Rescue	Part Rescue
Anti-CF45 antibodies	No Rescue	No Rescue	No Rescue
Countin KO Conditioned Medium	No Rescue	No Rescue	No Rescue
1mM glucose	No Rescue	Rescue	Rescue
Caffeine	No Rescue	Rescue	Rescue
cAMP pulsing	No Rescue	No Rescue	No Rescue
8-Br-cAMP	No Rescue	No Rescue	No Rescue
Anti-AprA, anti-CfaD antibodies	No Rescue	No Rescue	No Rescue
tert KO Conditioned Medium	No aggravation (i.e. 8h delay typical of *tert* KO)	Aggravation	Aggravation

Green shading indicates full or partial rescue of normal (wild-type) levels or activity by a treatment applied to *tert* KO cells. Red shading indicates no rescue. The final row refers to an attempt to exacerbate the *tert* KO phenotype.

https://doi.org/10.1371/journal.pgen.1008188.t002

Table 3. Attempts to phenocopy the *tert* KO phenotype in wild-type *Dictyostelium* cells.

	Timing of delay to aggregation	Streaming and aggregation	Mound and fruiting body size
tert KO Conditioned Medium	Phenocopies *tert* KO (but delay is only 2h)	Phenocopies *tert* KO	Phenocopies *tert* KO
tert KO cells (90–50%)	Normal	Phenocopies *tert* KO	Phenocopies *tert* KO
200 uM iron	Normal	Phenocopies *tert* KO	Phenocopies *tert* KO
BIBR 1532	Normal	Phenocopies *tert* KO	Phenocopies *tert* KO
MST 312	Normal	Phenocopies *tert* KO	Phenocopies *tert* KO
tert KO Conditioned Medium added to WT cells of other dictyostelids	Normal	Normal	Normal

Red shading indicates full or partial phenocopying of the *tert* KO phenotype by a treatment applied to wild-type cells. Green shading indicates that no phenocopying occurred.

https://doi.org/10.1371/journal.pgen.1008188.t003

we treated wild-type cells with structurally unrelated TERT specific inhibitors, BIBR 1532 (100nM) and MST 312 (250nM). BIBR 1532 is a mixed type non-competitive inhibitor, whereas MST 312 is a reversible inhibitor of telomerase activity (see Methods). Both inhibitors strikingly phenocopied two features of the *tert* mutant, in that we observed large early aggregate streams that broke and eventually resulted in mounds (Fig 4B; Table 3) and fruiting bodies that were small. The developmental delay, however, was not induced. Since the two inhibitors phenocopied the *tert* KO to a remarkable degree, it is likely that the inhibitor binding sites of *Dictyostelium* TERT are conserved. Human TERT [87], which shares a 23% homology with *Dictyostelium* TERT, failed to rescue the *tert* KO phenotype (S6 Fig). Surprisingly, the morphologies of TERT-overexpressing lines in the wild-type did not show any significant difference to those of the untreated wild-type (Fig 4A).

Overall, these results strongly support the idea that the relevant changes in the *tert* KO involve *tert* itself. The fact that the TERT inhibitors induced only two of the three *tert* KO defects is interesting. Given the lack of any apparent interconnection between the pathway that regulates the switch to aggregation, and that regulating mound size, it seems likely that TERT acts on more than one molecular target. It could be that the inhibitors do not perturb that part of TERT that interacts with the target that regulates the switch to development.

## Roles of components of the mound size regulation pathway in the *tert* KO: *smlA*, *CF*, *countin* and glucose

smlA and countin. Compared to the wild-type, in the *tert* KO cells, *smlA* and *countin* expression levels were, respectively, low and high (Fig 5A and 5B; Table 1). Also, Western blots performed with anti-countin antibodies showed higher *countin* expression in *tert* KO cells, compared to wild-type (Fig 5C). When *tert* was overexpressed in the *tert* KO background, both *countin* and *smlA* expression levels were returned to those of the wild-type (Fig 5A and 5B). This overexpression also rescued all the defects of the *tert* KO phenotype (Fig 4A; Table 2). Given the previously proposed regulatory relationship between *smlA* and *countin* (Fig 1; [28, 30, 32]), the most parsimonious explanation for the majority of the results reported so far in this study, is that one role of *tert* in *D. discoideum* is to promote the expression of *smlA*, thus indirectly inhibiting *countin* expression, and thus increasing glucose levels and mound/fruiting body size. This would suggest that *tert* could be one of the regulators of mound size.

The likelihood of some involvement of CF itself was supported by the effects of antibodies that target its components. When *tert* KO cells were treated with anti-countin or anti-CF50

A
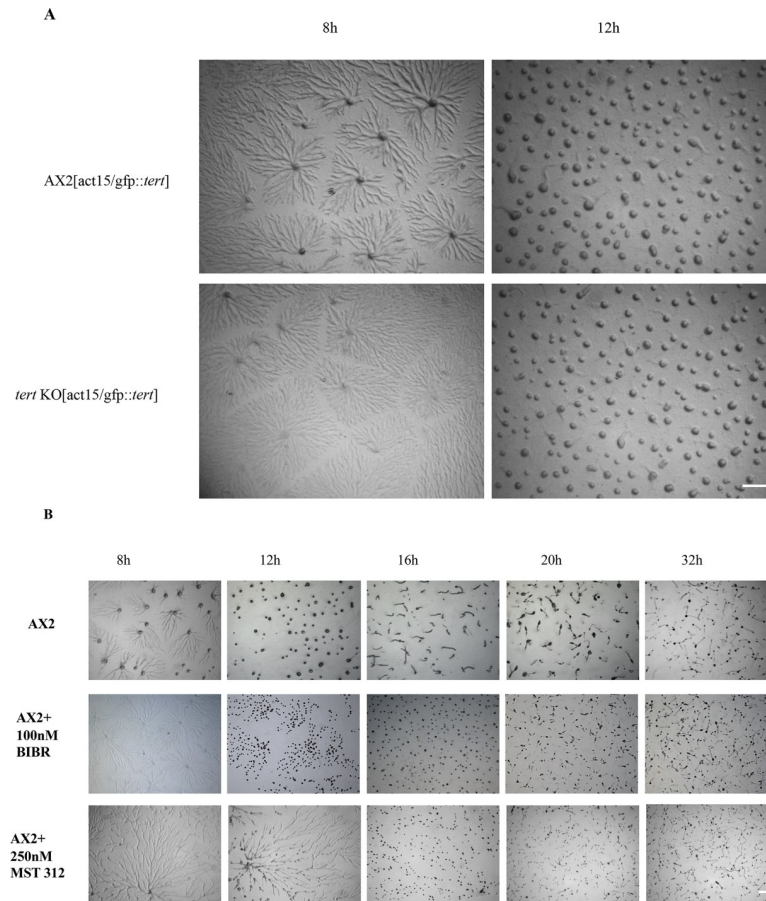
Fig 4. (A) Overexpression of TERT (act15/gfp::*tert)* rescued *tert* KO phenotype. Scale bar: 0.5 mm; (n = 3). (B) AX2 cells treated with 100 nM BIBR 1532 or 250 nM MST 312 in KK$_2$ buffer and developed on KK$_2$ agar phenocopied the *tert* KO streaming phenotype. The time points in hours are shown at the top. Scale bar: 0.5 mm; (n = 3).

https://doi.org/10.1371/journal.pgen.1008188.g004
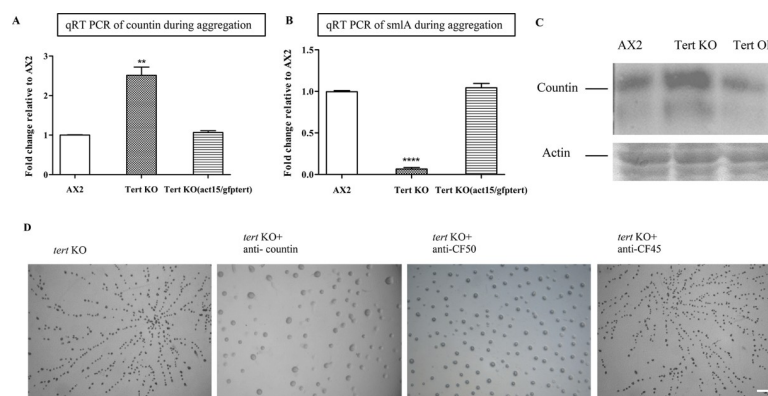
Fig 5. *Tert* regulates the levels of CF. qRT-PCR of (A) *countin* and (B) *smlA* during aggregation in AX2, *tert* KO and *tert* KO [act15/gfp-tert]. *rnlA* was used as mRNA amplification control. Level of significance is indicated as *p<0.05, **p<0.01, ***p<0.001, and ****p<0.0001; (n = 3). (C) Western blots with anti-countin antibodies. The gels were stained with Coomassie to show equal loading; (n = 3). (D) Cells were starved and developed with anti-countin, CF50 and CF45 antibodies (1:300 dilution) on KK$_2$ agar plates. Addition of anti-countin and anti-CF50 antibodies rescued *tert* KO group size defect. Scale bar: 0.5 mm; (n = 3).

https://doi.org/10.1371/journal.pgen.1008188.g005

antibodies (1:300 dilution), there was a reduction in aggregate fragmentation resulting in larger mounds compared to untreated *tert* KO controls (Fig 5D; Table 2); the development delay was not rescued. Adding anti-CF45 antibodies did not rescue any of the defects (Fig 5D; Table 2).

Indirect evidence that *tert* is acting upstream of CF was seen in the lack of effect of adding BIBR 1532 to *countin* KO cells, which typically exhibit no stream breaking and large mounds [30]. While, as noted above, BIBR 1532 leads to stream breaking and small mounds in wild-type cells, it did not lead to any change in the usual phenotype of *countin* KO cells (e.g. Fig 6A), which argues against *tert* acting downstream of *countin*.

Beyond the observations already noted, a range of other observations support the idea that some of the *tert* KO's features are due to the increased activity of a secreted mound-size regulating factor, such as countin. Conditioned medium (CM) from *tert* KO cells induced stream breaking in the wild-type (Fig 6B; Table 3) and led to reduced mound size. Also, adding *tert* KO CM to the *tert* KO itself aggravated the fragmentation phenotype (Fig 6B; Table 2). *Tert* KO CM was even capable of inducing stream fragmentation (Fig 6A), and reducing mound size, in *countin* mutants, suggesting that the CF levels of the *tert* KO CM were high. In each of these three cases, the *tert* KO CM not only affected streaming and mound size, but also induced, or aggravated, a development delay (Fig 6A and 6B; Tables 2 and 3). This suggests that the unknown TERT-induced factor that affects the developmental switch is also secreted.

Further, the presence of *tert* KO cells, even at very low concentrations (10%), was able to partially induce the *tert* KO phenotype when added to a population of wild-type cells and plated at an overall density of $5x10^5$ cells/cm^2 (Fig 6C; Table 3). The apparent potency of the presumed high CF levels produced by the *tert* KO cells might partly explain one otherwise unexpected observation: Adding wild-type CM to *tert* KO cells did not rescue any of their defects (Fig 6B; Table 2). While the wild-type CM in this case would be expected to act as a diluent of CF (and thus potentially rescue the *tert* KO), this effect would only be brief. Development occurs over many hours, during which time the *tert* KO conditions could allow the build-up of CF back to mound-size-limiting levels. Similar reasoning might also explain why CM from *countin* KO cells *(*which exhibit undelayed aggregation and normal streaming) did not rescue any of the defects of *tert* KO cells (Fig 6A; Table 2).

To determine if TERT plays a similar role in tissue size regulation in other dictyostelids, we checked if *tert* KO CM also affected the aggregate and mound sizes of other species (*D. minutum* and *D. purpureum*, each representing a distinct group in the dictyostelid taxonomy). The CM of *tert* KO did not affect the aggregate or mound size of the species tested (S7 Fig; Table 3) suggesting that some of the factors regulating mound size may be species specific. The fact that *tert* KO CM did not show any effect on other dictyostelids suggests that the countin-mediated effect may be species specific.

Glucose rescued streaming and mound size defects, but not the delay. As per the model shown in Fig 1, one of the downstream effects that should be seen if the *tert* KO has higher levels of CF, is the lowering of glucose levels. Glucose levels during aggregation were measured and in the *tert* KO were significantly lower (10.7±0.6 mg/ml) compared to wild-type (15.5 ±0.94 mg/ml) (Fig 7A, p = 0.0015). Supplementing 1 mM glucose rescued the aggregate streaming (and mound size), defects of the *tert* KO (Fig 7B), but not, as expected, the delay (Table 2).

Antibodies against AprA and CfaD did not rescue the *tert* KO phenotype. Previous work has shown that deletion of AprA and CfaD genes, involved in a different cell-density sensing pathway to that involving *smlA* and countin, leads to changes in mound-size [31], but, here, antibodies against AprA and CfaD did not rescue the KO phenotype (S8 Fig), suggesting,
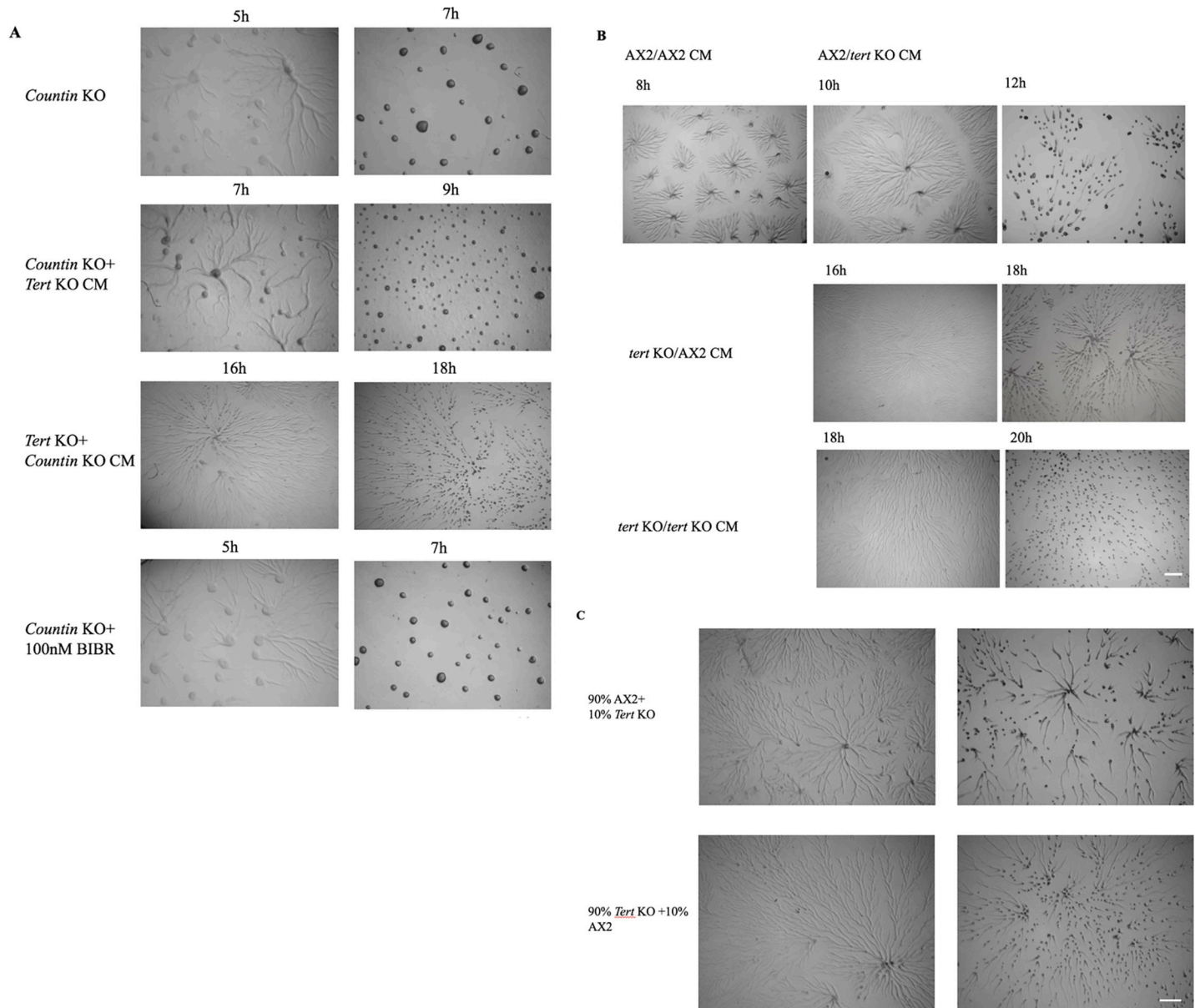
Fig 6. *Tert* regulates the levels of CF. (A) *Countin* KO cells were developed on KK$_2$ agar plates in the presence of *tert* KO conditioned media or BIBR1532. Scale bar: 0.5 mm; (n = 3). (B) Development in the presence of conditioned medium on KK$_2$ agar. *Tert* KO-CM induced stream breaking in AX2. (C) Reconstitution of AX2 in 1:9 ratio with *tert* KO did not rescue the stream breaking. Scale bar: 0.5 mm; (n = 3).

again, that impaired mound size determination in the *tert* KO is largely due to defective CF signal transduction.

Roles of cAMP and cAMP-related processes and factors in the *tert* KO

Given the perturbations seen in the *tert* KO, one would predict some abnormalities associated with cAMP dynamics [44–46, 88–90]. The role of cAMP in streaming, in particular, has been much studied. Below we examine how various cAMP processes or factors, related to streaming and developmental delay, were affected in the *tert* KO.
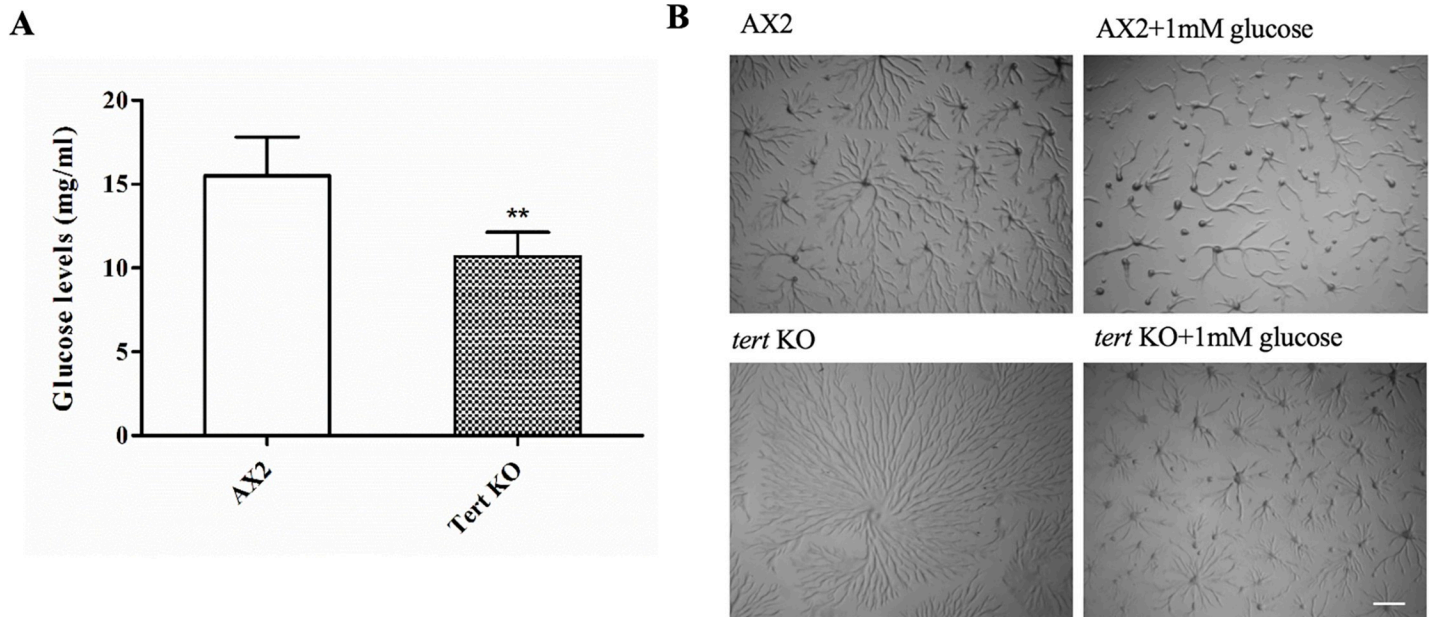
Fig 7. Effect of glucose on *tert* KO aggregate size. (A) Glucose levels during aggregation; (n = 3). (B) Wild-type AX2 and *tert* KO cells were developed on KK_2 agar plates in the presence of 1 mM glucose. Glucose rescues the streaming defect of *tert* KO. Scale bar: 0.5 mm; (n = 3). Level of significance is indicated as *p<0.05, **p<0.01, ***p<0.001, and ****p<0.0001.

Multiple cAMP wave generating centres observed in the *tert* KO. Starving cells normally aggregate by periodic synthesis and relay of cAMP, resulting in the outward propagation of cAMP waves from the aggregation centres [91]. We visualized cAMP waves by recording the time-lapse of development and then subtracting the image pairs [92]. Coordinated changes in cell shape and movement of cAMP waves can be indirectly visualized by dark field optics because of the differences in the optical density of cells moving/not moving in response to cAMP. Compared to the wild-type, which had a single wave generating centre, the *tert* KO had multiple wave propagating centres in a single aggregation territory (Fig 8, S9 Fig, S4 and S5 Videos). When the *tert* KO was rescued by overexpression of wild-type *tert*, so was the single
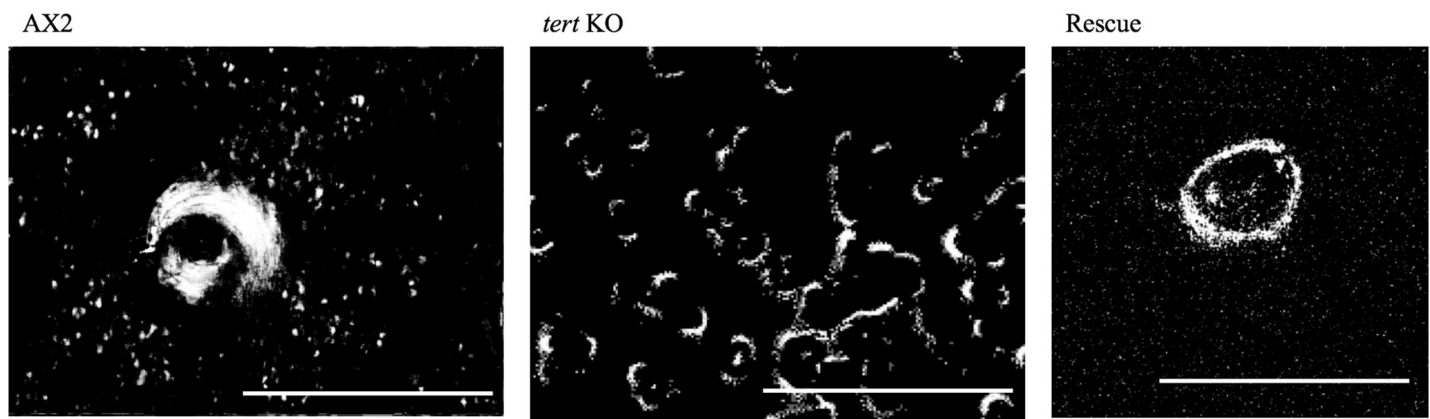
Fig 8. cAMP wave generating centres. Optical density wave images depicting wave generating centres in AX2, *tert* KO and a rescue strain are shown. AX2 and the rescue strain have a single wave generating centre, whereas *tert* KO has multiple wave generating centres in a single aggregate territory. Scale bar: 1 mm; (n = 3).
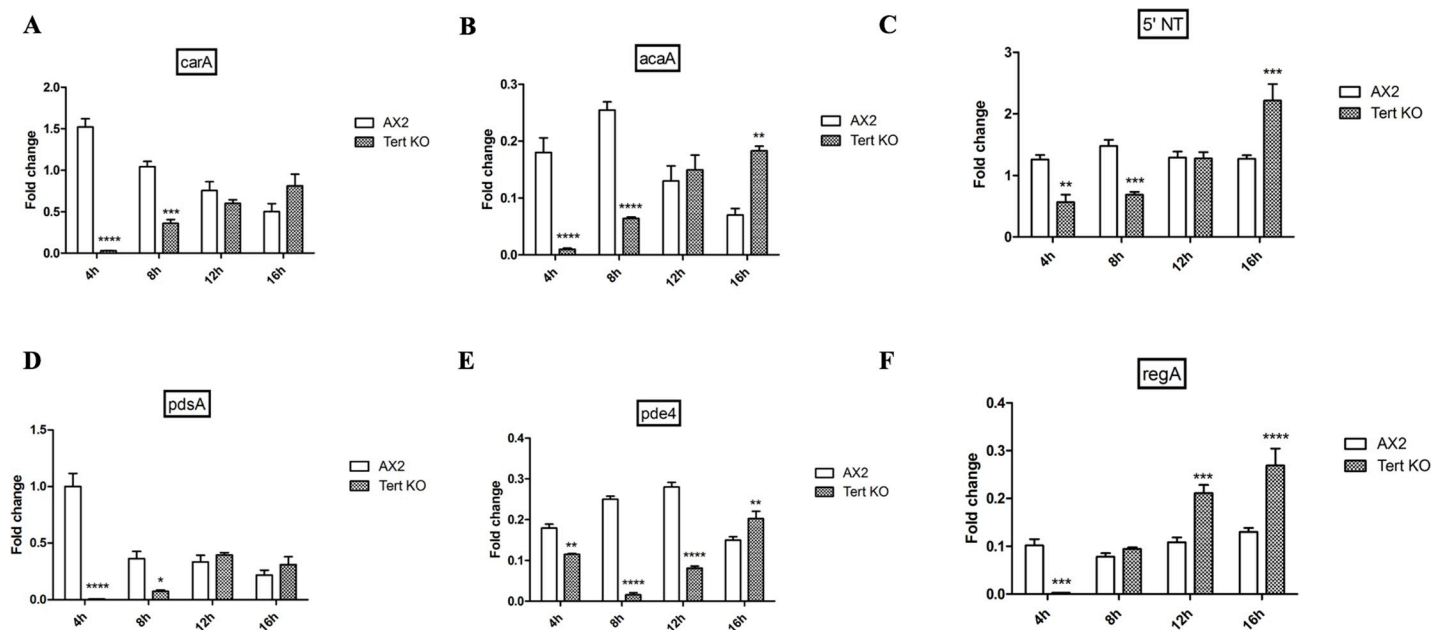
Fig 9. Delayed development in *tert* KO. (A-F) qRT-PCR of genes involved in the cAMP relay. Down-regulation of genes involved in the cAMP relay in *tert* KO. Fold change in mRNA expression at the indicated time points. *rnlA* is used as an mRNA amplification control; (n = 3). Level of significance is indicated as *p<0.05, **p<0.01, ***p<0.001, and ****p<0.0001; (n = 3).

wave propagating centre. The optical wave density analysis suggests that cAMP wave propagation is defective in *tert* KO, also contributing to stream breaking.

cAMP-related gene expression, cAMP levels, chemotaxis and relay were also impaired in the *tert* KO. Both the switch to aggregation, and normal streaming, require that a great variety of other cAMP-related processes occur properly. We quantified the relative expression of genes involved in cAMP synthesis and signaling in wild-type and *tert* KO cells by qRT-PCR. With respect to the switch to aggregation, the expression levels of *acaA* (cAMP synthesis), *carA* (cAMP receptor), *5'NT* (5' nucleotidase), *pdsA* (cAMP phosphodiesterases), *regA* and *pde4* were low initially but most started to 'recover' closer to the time that the *tert* KO manages to overcome its developmental delay (Fig 9A–9F). Another, perhaps more meaningful, approach is to compare the levels in the mutant and wild-type when they are at equivalent developmental stages. This was done at two stages (aggregation, stream breaking) for four of the cAMP genes (*acaA*, *carA*, *pdsA*, *pde4*). During aggregation (i.e. at 8 h in the wild-type; 16 h in the *tert* KO), *acaA* and *carA* expression levels were significantly lower in the mutant, and the other two genes trended lower (Fig 10A). During stream breaking (10 h; 18 h, respectively), only *acaA* was significantly lower (Fig 10B).

Correspondingly, at 8 h of development, cAMP levels were marginally lower in the *tert* KO (0.98±0.08 nM in the KO; 1.59±0.15 nM in wild-type; Fig 10C, p = 0.005). By 12 h, however, as the *tert* KO cells are closer to the time when their streaming will begin (i.e. 16 h) both cAMP-related gene expression, and cAMP levels increase, implying that the initially down-regulated expression of cAMP signaling might explain the long-delayed switch to aggregation in the *tert* KO. As to how cAMP-related genes or processes do recover in the absence of TERT, there are no indications in our results, but regulatory networks are well-known to exhibit a degree of robustness [93, 94].

As noted, cAMP-related gene expression levels of the *tert* KO lag behind that of the wild-type, and they increase as the mutant enters a similar developmental phase. When cAMP levels
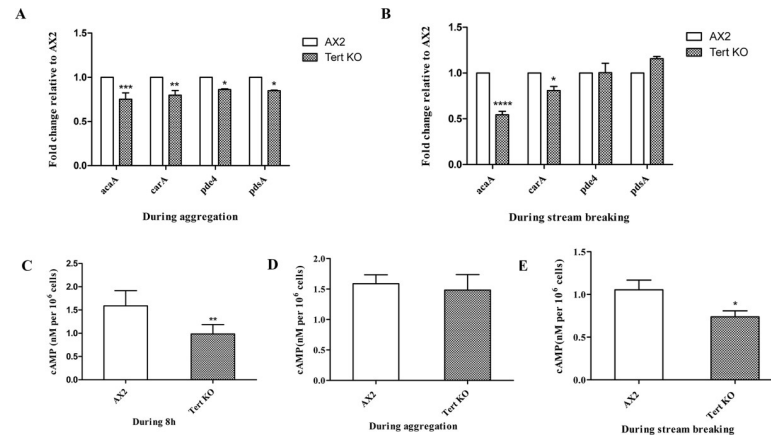
Fig 10. Defective cAMP relay of *tert* KO. cAMP relay and expression of *acaA*, *carA*, *pde4*, *pdsA* in *tert* KO during (A) aggregation and (B) stream breaking. Fold change in mRNA expression is relative to AX2 at the indicated time points. *rnlA* was used as an mRNA amplification control, (n = 3). cAMP levels in *tert* KO during (C) 8 h of development in AX2 and *tert* KO, (D) aggregation, (E) stream breaking. Level of significance is indicated as *p<0.05, **p<0.01, ***p<0.001, and ****p<0.0001; (n = 3).

were quantified during aggregation and stream breaking using an ELISA-based competitive immunoassay, the cAMP levels in the wild-type and *tert* KO were 1.59±0.15 nM and 1.48±0.25 nM, respectively, during aggregation (Fig 10D, p = 0.73); and 1.05±0.11 nM and 0.74±0.70 nM during stream breaking (Fig 10E, p = 0.04). Thus, these lower absolute levels of cAMP in the *tert* KO may also contribute to abnormal stream breaking, with the amoebae unable to relay signals to their neighbours.

To test whether cAMP-based chemotaxis was normal, we performed an under-agarose chemotaxis assay, towards 10 μM cAMP. The trajectories of cells were tracked and their chemotaxis parameters were quantified. Although the speed of cells towards cAMP was higher in *tert* KO (16.01±1.39 μm/min) compared to the wild-type (12.74±0.43 μm/min), the directionality was significantly reduced in *tert* KO cells (0.37±0.03 compared to 0.59±0.04). The chemotactic index of *tert* KO cells also was lower (0.63±0.05) compared to wild-type cells (0.82±0.06) (Fig 11A–11C).

The chemotaxis defect of *tert* KO was not rescued by cAMP pulsing or 8-Br-cAMP. To gain further insights into the streaming defect of the *tert* KO cells, we examined if cAMP pulsing could rescue the chemotaxis defect [95, 96]. cAMP (50nM) pulsing was carried out every 6 minutes for 4 hours and thereafter, the cells were seeded in the starvation buffer at a density of 5×10^5 cells/cm^2 and different developmental stages were monitored (Fig 12A). The streaming defect of *tert* KO was not rescued by cAMP pulsing, suggesting that other components of cAMP signaling are necessary to rescue the defect.
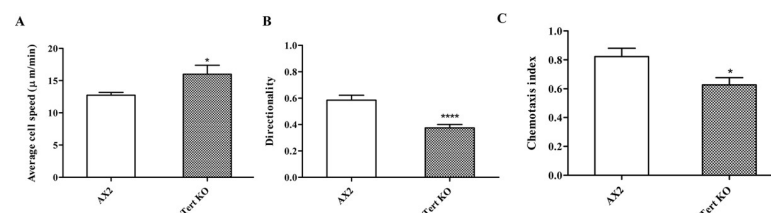
Fig 11. Defective cAMP chemotaxis of *tert* KO. Under-agarose cAMP chemotaxis assay in response to 10μM cAMP. (A) Average chemotaxis speed in response to cAMP. (B) directionality of chemotaxing cells and (C) chemotaxis index are shown. The graph represents the mean and SEM of 3 independent experiments.

A

B
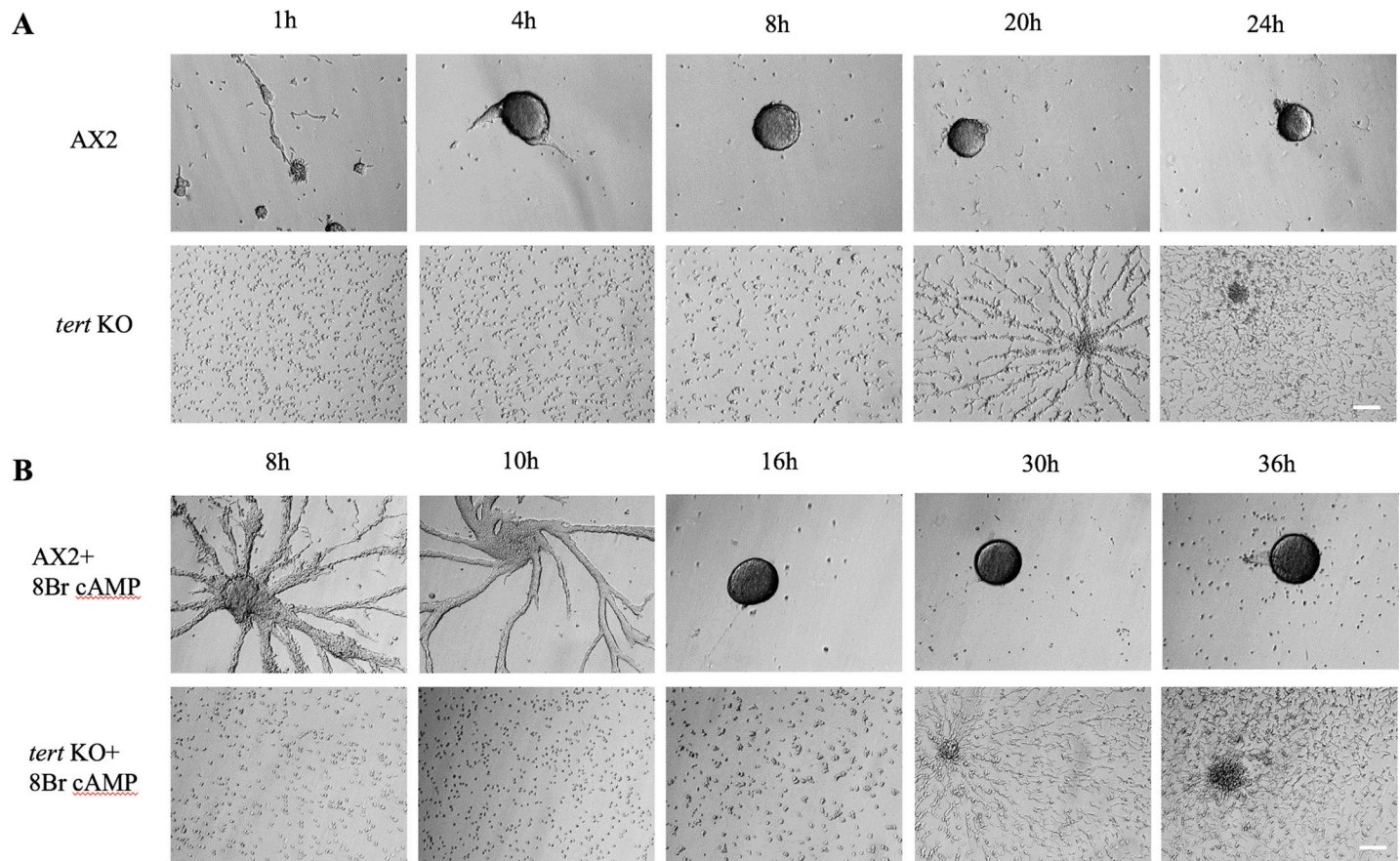
Fig 12. cAMP sensing in *tert* KO. (A) Wild-type and *tert* KO cells were starved for 1 hour and pulsed every 6 min with 50 nM cAMP for 4 h. Cells were then resuspended in BSS buffer and seeded at a density of 1×10^5 cells/ml, and observed under a microscope. (B) Wild-type and *tert* KO cells were washed in BSS buffer, seeded at a density of 1×10^5 cells/ml, and incubated in BSS or BSS + 5 mM 8-Br-cAMP for 5 h. Cells were washed and then observed under a microscope. Scale bar: 100 μm; (n = 3).

If cAMP receptor activity is compromised, that could also lead to defective signaling and to test this, we used a membrane-permeable cAMP analog 8-Br-cAMP. This has a poor affinity for extracellular cAMP receptors and enters the cells directly [47]. Cells were incubated with 5mM 8-Br-cAMP and after 5 h, the cells were transferred to Bonner's Salt Solution and development was monitored (Fig 12B). If 8-Br-cAMP had rescued the *tert* KO's defects, this would have suggested an impairment of cAMP receptor function, but this was not observed. Thus, impaired function of the receptor might not be responsible for the *tert* KO's chemotactic defects. However, it is also possible that the receptor is impaired but retains enough activity to obscure any effects of 8-Br-cAMP.

High adenosine levels in the *tert* KO induced large aggregation streams. As mentioned previously, adenosine and caffeine are known to alter the cAMP relay [97, 98], thereby affecting aggregate size. This occurs in a number of dictyostelids [35]. We observed enhanced expression of *5'NT* in the *tert* KO (Fig 13A, p = 0.0042) suggesting increased adenosine levels (5'NT converts AMP to adenosine). Hence, adenosine levels were quantified and these were significantly higher (235.37±26.44 nM/10^6 cells) in *tert* KO cells compared to wild-type (35.39 ±12.78 nM/10^6 cells) (Fig 13B, p = 0.0051). The adenosine antagonist, caffeine (1 mM), rescued the streaming defect (Fig 13C), and restored the mound size, suggesting that excess adenosine in the *tert* KO causes larger streams. It did not, however, rescue the developmental delay.
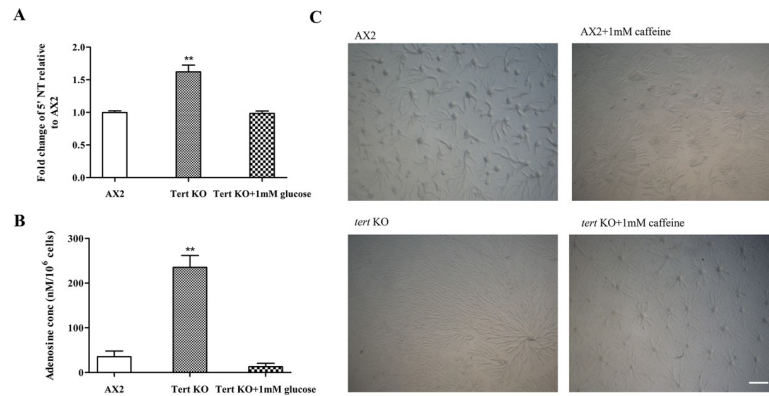
Fig 13. Effect of adenosine on aggregate size. (A) qRT-PCR of 5'NT. Fold change in mRNA expression is relative to AX2 at indicated time points. *rnlA* is used as mRNA amplification control; (n = 3). (B) Quantification of adenosine levels. Level of significance is indicated as $^*p<0.05$, $^{**}p<0.01$, $^{***}p<0.001$, and $^{****}p<0.0001$; (n = 3). (C) Cells were developed on KK_2 agar plates in the presence of 1 mM caffeine; *tert* KO streaming defect was rescued. Scale bar: 0.5 mm; (n = 3).

https://doi.org/10.1371/journal.pgen.1008188.g013

Since glucose also rescues the streaming defect in *tert* KO cells, adenosine levels were quantified subsequent to treating with 1 mM glucose. Glucose treatment reduced adenosine levels (13.07 ± 7.51 nM/10^6 cells) in *tert* KO cells to a level that is more comparable to wild-type cells (35.39 ± 12.78 nM/10^6 cells), but as already noted, it did not rescue the developmental delay. Importantly, *5'NT* expression and adenosine levels reduced significantly subsequent to stream breaking (S10 Fig). This could perhaps be due to negative feedback on *tert* itself.

Streaming defects of the *tert* KO were not due to increased iron levels. *Dictyostelium* cells, when grown in the presence of 200 μM iron, formed large streams that fragmented into multiple mounds, strikingly resembling the *tert* KO phenotype [99]. As the phenotypes had similarities, we examined if TERT mediates its effect by altering intracellular iron levels. We quantified iron by ICP-OES and the levels were not significantly different between the wild-type (16.38 ± 1.21 ng/10^7 cells) and *tert* KO cells (15.25 ± 0.81 ng/10^7 cells) (S11 Fig, p = 0.4573), suggesting that *tert* KO phenotype is not due to altered iron levels.

The role of adhesion-related factors in the *tert* KO, as they affect streaming and mound size

Cell-substratum adhesion is also important for migration and proper streaming. By shaking cells at different speeds (0, 25, 50 and 75 rpm), it is possible to vary substratum dependent sheer force. Thus, by counting the fraction of floating cells at different speeds, it is possible to check substratum dependent adhesion. Although both wild-type and *tert* KO cells exhibited a sheer force-dependent decrease in cell-substratum adhesion, *tert* KO cells exhibited a significantly weaker cell-substratum adhesion (S12 Fig, p<0.0001), affecting cell motility in a way that might also contribute to stream breaking.

Cell-cell adhesion is also an important determinant of streaming and mound size in *Dictyostelium* [41]. To examine if adhesion is impaired in the mutant, we checked the expression of two major cell adhesion proteins, *cadA*, expressed post-starvation (2 h) and *csaA* expressed during early aggregation (6 h). *cadA*-mediated cell-cell adhesion is Ca^{2+}-dependent and thus EDTA-sensitive, while *csaA* is Ca^{2+} independent and EDTA-resistant [67]. Both *csaA* and *cadA* expression were significantly down-regulated (Fig 14A and 14B).

Further, cell adhesion was monitored indirectly by counting the fraction of single cells not joining the aggregate. Aggregation results in the gradual disappearance of single cells and thus
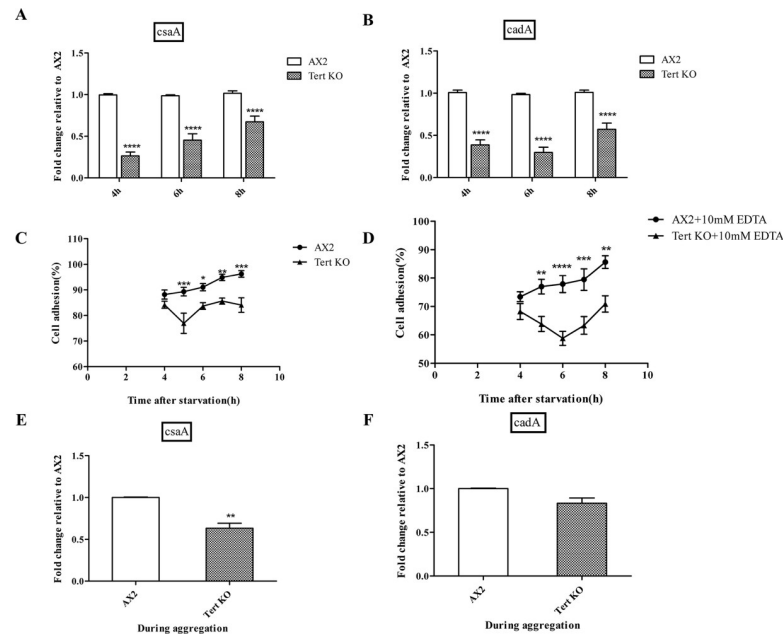
Fig 14. Disruption of *tert* affects cell adhesion. qRT-PCR of (A) *csaA* and (B) *cadA*. *rnlA* was used as mRNA amplification control. Wild-type and *tert* KO cells were starved in Sorensen phosphate buffer at 150 rpm and 22˚C. Samples were collected at the start of the assay and at one-hour time points after 4 h of starvation. Percentage of cell adhesion plotted over time. (C) EDTA resistant cell-cell adhesion, (D) EDTA sensitive cell-cell adhesion. Level of significance is indicated as *p<0.05, **p<0.01, ***p<0.001, and ****p<0.0001. (E) *csaA* levels and (F) *cadA* levels during aggregation; (n = 3).

it is possible to measure aggregation by determining the ratio of single cells remaining. To examine Ca^{2+}-dependent cell-cell adhesion, the assay was performed in the presence of 10 mM EDTA. Both EDTA-sensitive and resistant cell-cell adhesion were significantly defective in *tert* KO cells (Fig 14C, p = 0.0033 and 14D, p = 0.0015). The levels of *csaA* and *cadA* were also lower in the *tert* KO during aggregation when compared to the WT (Fig 14E, p = 0.0037 and 14F, p = 0.0508). Thus, the delay in *tert* KO development might be the basis for differences in gene expression.

These results imply that defective cell-substratum and cell-cell adhesion might play roles in the abnormal streaming and mound-size regulation of the *tert* KO.

The developmental delay of the *tert* KO was associated with reduced polyphosphate levels

One interesting observation was that the only treatment that fully rescued the *tert* KO cells was the overexpression of wild-type *tert*. Also, the only other treatment that rescued the developmental delay itself was mixing wild-type cells with the *tert* KO cells at a 1:1 ratio (Fig 15; Table 2). Even though caffeine and glucose rescued streaming and mound size, and apparently this was at least partly mediated via their impact on cAMP-regulated processes, neither of the compounds rescued the delay, even though abnormalities of cAMP-regulated processes are commonly reported causes of delay in other *Dictyostelium* studies [44–46].

Thus, we examined polyphosphate levels in the *tert* KO because of their known importance to developmental timing in *Dictyostelium* [43]. We stained the CM with DAPI for 5 minutes and checked the polyphosphate specific fluorescence using a spectrofluorometer. The CM of *tert* KO cells has reduced polyphosphate levels (49.55±2.02 µM) compared to wild-type (60.62

16h	14h	8h
90% *tert* KO+ 10% AX2	80% *tert* KO+ 20% AX2	50% *tert* KO+ 50% AX2
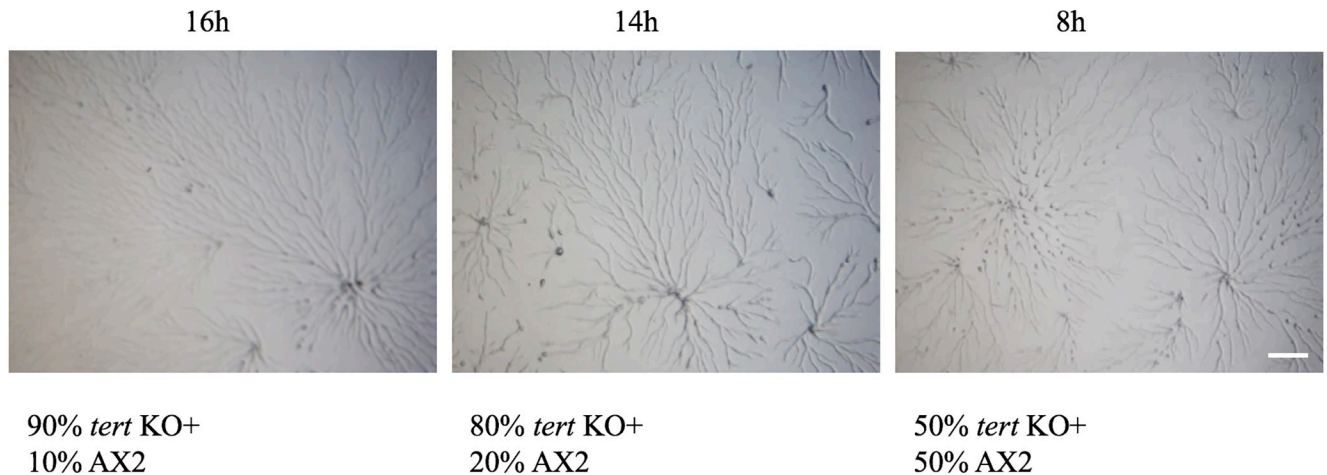
Fig 15. Rescue of delay by added wild-type cells. Wild-type AX2 and *tert* KO were reconstituted at 1:9, 2:8 and 1:1 ratio and developed on KK_2 agar. Developmental delay of *tert* KO was rescued by AX2 at 1:1 ratio. Scale bar: 0.5 mm; (n = 3).

$\pm 1.95\ \mu M$), implying that low polyphosphate levels might also contribute to the delay in initiating development in this system (Fig 16, $p = 0.0009$).

Conclusions

Our results reveal that TERT plays an important role in many aspects of *Dictyostelium* development. The *tert* KO exhibited a wide range of developmental defects. Despite suitable environmental conditions for multicellular development to begin, the start of the streaming phase is delayed by 8 h. Having once begun, development proceeds and ends abnormally, with large streams, uneven fragmentation, and, eventually, small mounds and fruiting bodies. The wide-ranging developmental defects are associated with changes to the levels, or expression, of
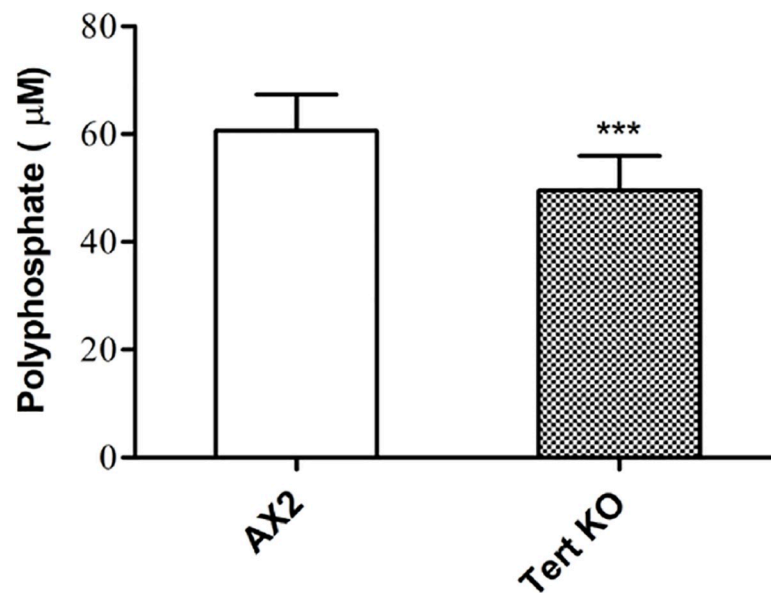
Fig 16. Polyphosphate levels were low in the *tert* KO. Polyphosphate levels in conditioned media of AX2 and *tert* KO. Level of significance is indicated as $^*p<0.05$, $^{**}p<0.01$, $^{***}p<0.001$, and $^{****}p<0.0001$; (n = 3).
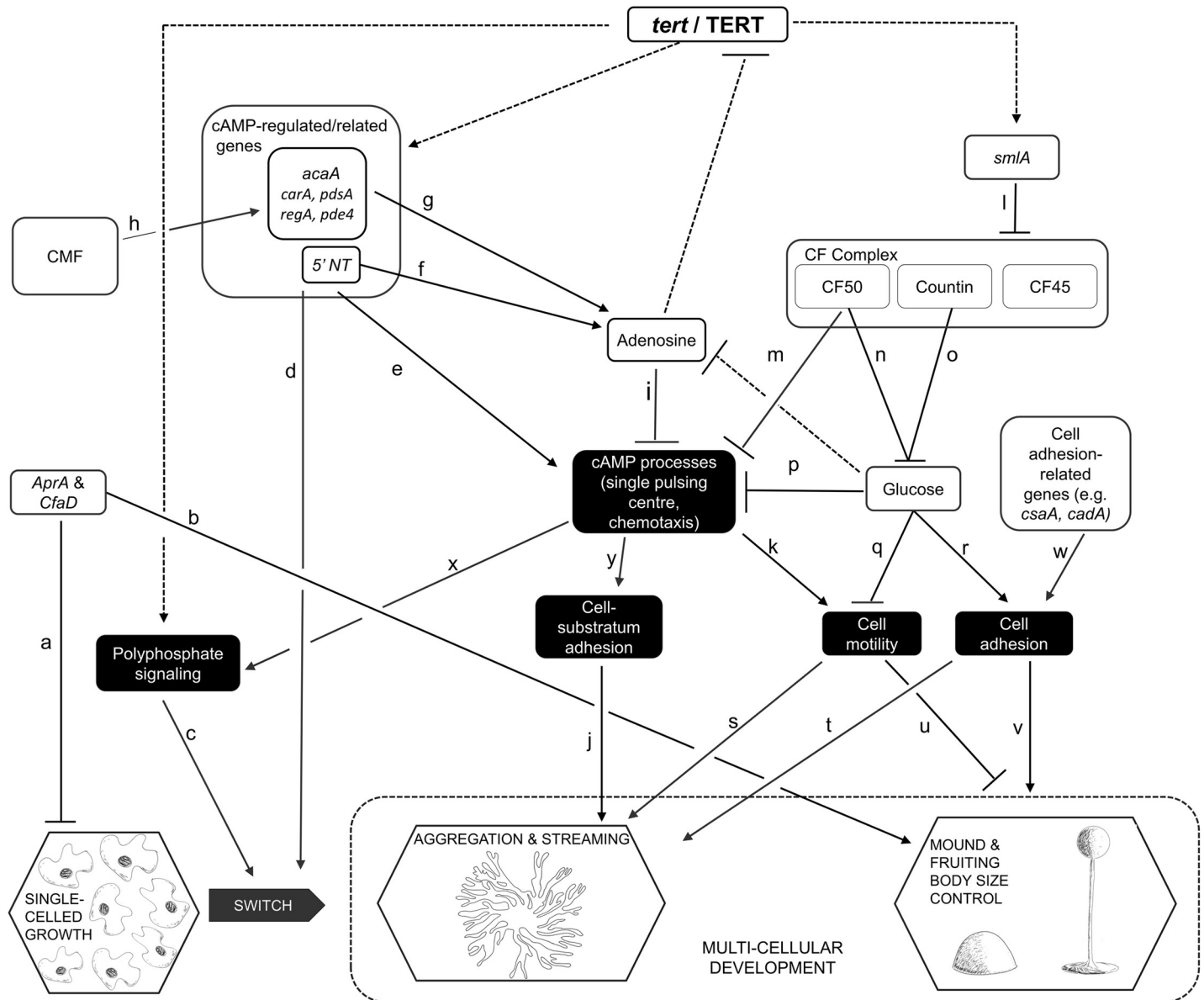
Fig 17. Some of the possible targets of *tert*/TERT in development of *D. discoideum*, as indicated by this study. This work, the first functional study of a telomerase in *Dictyostelium*, revealed that TERT influenced many previously reported developmental processes and pathways. The dashed lines represent effects previously unreported, involving multiples phases of the life-cycle. Adenosine, however, was found to provide negative feedback on *tert* expression. The letters next to the undashed lines are explained in the caption of Fig 1.

genes and compounds that are known to be highly upstream regulators of the various stages of development, such as streaming and mound/fruiting body formation. Based on the perturbations in the *tert* KO, and our other experiments, Fig 17 depicts the possible extent of processes, and potential mediating factors, that might depend upon normal *tert* expression/TERT activity in the wild-type. Note that the arrows that connect *tert*/TERT to any element in the diagram are not meant to suggest that TERT directly regulates that element, only that TERT is important, perhaps in some indirect way, for the normal levels, or activity, of that element.

One of the most striking findings was that TERT appears to regulate, or is at least necessary for, the normal activity of what was previously known as the most upstream regulator of

mound size, *smlA* [28, 30, 32]. Expression levels of *smlA* were reduced in the *tert* KO, and we also observed a wide variety of the expected downstream effects of lowered *smlA* levels. All of these, and a wide variety of treatments that rescued the size-defect of the mutant phenotype, support the idea that the reduction of mound size in the *tert* KO was indeed mediated via the abnormal functioning of the previously-identified elements of the mound-size regulation pathway.

In addition to the rescue approach, treatments that attempted to phenocopy the *tert* KO phenotype in the wild-type, also suggest TERT is one of the upstream regulators of mound size. In particular, given that size regulation in *D. discoideum* depends upon secreted factors of the CF complex, one would have predicted the effects we observed when *tert* KO CM was added to wild-type cells. Another strong indication that *tert* acts upstream, at least of CF, was that the inhibition of *tert* activity in *countin* mutants failed to phenocopy the *tert* KO phenotype.

A similarly rich range of results (involving the *tert* KO phenotype, and its rescue, and phenocopying) support the idea that TERT also plays a high-level role in the regulation of streaming. During the streaming phase, two genes associated with cAMP related-processes in *D. discoideum* (*acaA*, *carA*) were significantly downregulated (compared to the wild-type), and the levels of several other genes trended lower. This was also accompanied by lower cAMP levels. This might explain the defective chemotaxis and cell motility of the *tert* KO.

Of course, the regulation of streaming is not entirely isolated from that of size. Glucose, one of the central elements of the CF pathway, influences several cAMP-related processes [64]. Thus, it was not surprising that adding 1 mM glucose to the *tert* KO cells rescued both the size and streaming defects. This study, however, provided a new insight into how the rescue of streaming occurs, because added glucose also reduced adenosine levels. Thus, in the *tert* KO, the low glucose levels might lead to higher adenosine levels, allowing it to inhibit cAMP related processes (via pathway i, Fig 17). In normal development, given the known sequence of the telomere repeats of *D. discoideum* (A-G$_{(1-8)}$; [74]), and the fact that telomerase activity would therefore recruit cellular stores of adenosine, it is possible that normal TERT activity keeps adenosine levels low. As yet, however, whether TERT actually acts as a functional telomerase in *D. discoideum* is not known.

The *tert* gene we characterized includes the conserved domains and structure of a telomerase reverse transcriptase. Also, supplementing structurally unrelated but specific inhibitors of TERT to wild type cells phenocopies the mutant phenotype. The widely used method to test telomerase activity is the TRAP assay. However, this method failed to detect telomerase activity in *D. discoideum* and there may be both technical and innate limitations. For example, possible reasons for the lack of any observed activity are that: (i) the presence of rDNA palindrome elements in the chromosomal ends, suggesting a novel telomere structure and the possible role of TERT in maintaining both rDNA and chromosomal termini [74]. This could be an alternate pathway of telomere maintenance in *D. discoideum*; and (ii) polyasparagine repeats, present in the TERT protein of *Dictyostelium*, splitting the functional domain into two halves. For telomerase activity, a functional TERT is important in humans [100–102]. In yeast as well as humans, truncation of one of the TERT protein domains is known to abolish its function [103, 104]. While it is not yet clear whether the apparent absence of canonical TERT function in *D. discoideum* is due to the absence of normal eukaryote telomeres [105], other studies suggests that TERT is not always associated with telomerase activity. The silkworm genome contains a telomerase gene, but the telomerase itself displays little or no enzymatic activity [106, 107]. The telomeres of silkworm consist of the telomeric repeats typical of insects, but also harbor many types of non-LTR retrotransposons [106, 108, 109]. Also of interest is that species of Calcarea (sponges), Cnidaria (sea anemones and jellyfish) and Placozoa, all have metazoan

telomeric sequences, but display little or no telomerase activity [110]. *D. discoideum* might employ an alternative mode of telomere addition, such as the recombination seen in yeast [111] or the retrotransposition of *Drosophila* [112, 113].

The discussion so far, while it establishes that TERT is needed for several developmental processes to take place, does not help to distinguish whether or not it acts more than once, or if it has more than one target. Could TERT for example act more like the much studied homeodomain proteins, master regulators of animal development, but which only act during very early embryological life [114, 115]? Likewise, in *D. discoideum*, CMF appears to act only once [34]. Two lines of argument suggest that TERT is different.

First, the biphasic nature of *tert*'s expression pattern suggest that it could possibly act during two stages of development. In the wild-type, *tert* expression builds up to its first peak at 8 h, thus being a potential candidate for enabling streaming to begin, and to proceed correctly, around this time. It then dips markedly to a low point at 10 h, whereby it might help to enable stream break-up by its relative absence. Then, it begins its climb to its second peak at 12 h, when mound size is being finalised. However, it is also possible that the later-occurring defects seen in the *tert* KO correspond to pleiotropic effects of TERT being absent at a much earlier time-point.

Second, while it is well known that cAMP-related processes play important roles in allowing streaming to begin and to proceed properly, and while we have shown that TERT influences multiple cAMP related processes, the pathway by which TERT influences the initiation of streaming seems distinct from that used for maintaining it. Both glucose and caffeine, for example, rescued the streaming and size defects of the *tert* KO, but the delay was unaffected. Complementarily, when wild-type cells were mixed at 50% with *tert* KO cells, they rescued the delay defect only. In fact, the only treatment that fully rescued the *tert* KO was the overexpression of wild-type *tert*.

Interestingly, MAP kinase kinase (MEK1) disruption results in a stream-breaking phenotype similar to the *tert* KO [56], suggesting that MEK1 could be involved in either CF secretion or signal transduction. Also, signals transmitted through p38 mitogen-activated protein kinase (MAPK) regulate hTERT transcription in human sarcoma [116]. We speculate that MEK1 might regulate countin levels through TERT, thus helping to regulate tissue size in *D. discoideum*.

Also, it is known that MST 312 (a TERT inhibitor) treatment reduces tumour size by 70% in a mouse xenograft model and this inhibition preferentially targets aldehyde dehydrogenase-positive cancer stem cell-like cells in lung cancer [117]. In *Dictyostelium*, disruption of aldehyde reductase increases group size [118] and, since aldehyde dehydrogenase and aldehyde reductase have opposing activities (oxidation and reduction of aldehydes respectively), they might have opposite functions in group size regulation as well. TERT might possibly be regulating aldehyde reductase activity in determining mound size in *D. discoideum*.

Other genes are also known to play a significant role in aggregate size determination in *Dictyostelium*, such as *dio3* [119] and *pkc* [120]. However, it is not known if they interact with TERT in determining mound size.

This study indicates for, the first time, that TERT acts in several non-canonical ways in *D. discoideum*, influencing when aggregation begins, the processes involved in streaming, and the eventual size of the fruiting body. TERT's influences appear to occur upstream of many other regulators of streaming and fruiting body size. Curiously, as yet we have no evidence that TERT acts as a canonical telomerase, nor is it known whether any other enzyme protects the unusually sequenced telomeres of this species. Given that telomere research is still in progress, we cannot even rule out that TERT's apparently non-canonical roles in *D. discoideum* development are in fact mediated via some as-yet unidentified action on its unusual telomeres. In the

most heavily studied stages of the organism's life-cycle, that is, those that occur in response to starvation, replication has ceased, so further study of this particular point should focus on the amoeboid stage. More generally, this study has revealed a previously unreported non-canonical process influenced by a telomerase, tissue size regulation. This role of TERT, together with its influence on cell motility and adhesion, and the levels of chalone-like secreted factors, bear consideration by those engaged in cancer research.

Methods

Dictyostelium culture and development

Wild-type *D. discoideum* (AX2) cells were grown with *Klebsiella aerogenes* on SM5 plates, or axenically, in modified maltose-HL5 medium (28.4 g bacteriological peptone, 15 g yeast extract, 18 g maltose monohydrate, 0.641 g Na_2HPO_4 and 0.49 g KH_2PO_4 per litre, pH 6.4) containing 100 units penicillin and 100 mg/ml streptomycin-sulphate. Cells were also grown in Petri dishes as monolayers. Other dictyostelid species (*D. minutum* and *D. purpureum*) were grown with *Klebsiella aerogenes* on SM5 plates and cells were harvested when there was visible clearing of bacterial lawns.

To trigger development, cells were washed with KK_2 buffer (2.25 g KH_2PO_4 and 0.67 g K_2HPO_4 per liter, pH 6.4) and plated on 1% non-nutrient KK_2 agar plates at a density of $5x10^5$ cells/cm^2 in a dark, moist chamber [121]. To study streaming, cells were seeded in submerged condition (KK_2 buffer) at a density of $5x10^5$ cells/cm^2.

BIBR 1532 is a specific non-competitive inhibitor of TERT with IC50 value of 93 nM for human telomerase [122]. To find the optimal dose response of BIBR 1532 in *Dictyostelium*, starved cells were plated in phosphate buffered agar with different concentrations of BIBR 1532 (10 nM, 25 nM, 50 nM, 100nM and 200 nM) and 100nM was found to be the minimal effective dose in inducing complete stream breaking. MST 312, which is structurally unrelated to BIBR 1532, is a reversible inhibitor of TERT with IC50 value of 0.67 μM for human telomerase [123]. The minimal effective dose in *Dictyostelium* was found to be 250 nM. Inhibitor treatments were carried out with freshly starved cells resuspended in KK_2 buffer and plated on KK_2 agar plates.

Telomerase activity assay (TRAP)

The TRAP assay takes advantage of the low substrate specificity of telomerase, and involves replacing the telomere sequence with a synthetic template. The telomerase first extends the synthetic substrate primer by adding telomere repeats and these primary products are further amplified by PCR. The primer must have certain modifications, such as an anchor sequence at the 5' end and two mismatches within the telomerase repeats [124, 125]. For the TRAP assay in *Dictyostelium*, we have used different primer sets (S2 Table) according to the basic design principles [124].

Generation of *tert* knockout (KO) in *D. discoideum* by homologous recombination

The KO vector for *tert* disruption was designed following standard cloning procedures. A 5' fragment of 678 bp and a 3' fragment of 322 bp spanning the *tert* gene (DDB_G0293918) and intergenic regions were PCR amplified and cloned on either side of a bsR cassette in pLPBLP vector (S13 Fig). Restriction endonuclease digestion and DNA sequencing were carried out to confirm the integrity of the KO vector. The *tert* KO vector was transfected to *D. discoideum* cells by electroporation. Axenically grown AX2 cells were washed twice with ice-cold

electroporation buffer and $1x10^7$ cells were resuspended in 100 μl EP^{++} buffer containing 10 μg of linearized *tert* KO vector. The cell suspension mixed with linearized KO vector was transferred to pre-chilled cuvettes (2 mm gap, Bio-Rad) and electroporated (300 V, 2 ms, 5 square wave pulses with 5 s interval) using a BTX ECM830 electroporator (Harvard Apparatus). The cell suspension was then transferred to a Petri dish containing 10 ml of HL5 medium and incubated at 22°C. After 24 h, the cultures were replaced with fresh HL5 supplemented with 10 μg/ml blasticidin (MP Biomedicals). Blasticidin-resistant clones were screened after three days. Genomic DNA isolated from *tert* KO clones were subjected to PCR analysis to confirm *tert* disruption using different primer combinations (S3 Table).

Construction of *tert* expression vector

Using genomic DNA as template, a 3.8kb *tert* sequence was PCR amplified using ExTaq polymerase (Takara) and ligated in pDXA-GFP2 vector by exploiting the HindIII and KpnI restriction sites. This vector was electroporated to *tert* KO and AX2 cells and G418 resistant (10 μg/ml) clones were selected and overexpression was confirmed by semi-quantitative PCR. Primer sequences used for generating the vectors are mentioned in S4 Table.

Conditioned medium assay

Conditioned medium was prepared as described previously with slight modifications [126]. Briefly, log phase cells of AX2 and *tert* KO were resuspended at a density of $1x10^7$ cells/ml and kept under shaking conditions for 20 h. Cells were pelleted and the supernatant was further clarified by centrifugation. The clarified supernatant (CM) was used immediately. To check the effect of CM on aggregate size, cells were developed in the presence of CM on non-nutrient agar plates and development was monitored. KK_2 buffer was used as control. To deplete extracellular CF with anti-countin antibodies, cells were starved in KK_2 buffer. After 1 h, the cells were developed with anti-countin antisera (1:300 dilution) in KK_2 buffer [65].

Western blot

To examine countin protein expression levels during aggregation, a Western blot was performed with anti-countin antibody. Cells were resuspended in SDS Laemmli buffer, and boiled for 3 min. Subsequently, the samples were run in a 12% SDS-polyacrylamide gel and Western blots were developed using an ECL Western blotting kit (Bio-Rad). Rabbit anti-countin antibodies were used at 1: 3000 dilution.

Cell-cell adhesion assay

Log phase cells were starved at a density of $1x10^7$ cells/ml in KK_2 buffer in shaking conditions at 22°C for 4 h. At the beginning of starvation, $4x10^7$ cells were removed and resuspended in 2 ml Sorensen phosphate buffer, vortexed vigorously and 0.4 ml of cell suspension was pipetted immediately in vials containing 0.4 ml ice-cold Sorensen phosphate buffer or 0.4 ml of 20 mM EDTA solution. The cell suspension was then transferred to a shaker and incubated for 30 min and 0.2 ml of 10% glutaraldehyde was added to each sample at the end of incubation and stored for 10 min. Then, 7 ml Sorensen phosphate buffer was added to each vial. Cell adhesion was indirectly measured by counting the number of single cells left behind using a hemocytometer [127].

Cell-substratum adhesion

To measure cell-substratum adhesion, $5x10^5$ cells were seeded in 60mm Petri dishes and incubated at 22°C for 12 h. The Petri dishes with the cell suspension was placed on an orbital shaker at different speeds (0, 25, 50, 75 rpm). After 1 h, adherent and non-adherent cells were harvested, counted using a hemocytometer and the fraction of adherent cells was plotted against the rotation speed [58].

Visualization of cAMP waves

To visualize cAMP wave propagation, $5x10^5$ cells/cm^2 were plated on 1% non-nutrient agar plates and developed in dark moist conditions at 22°C. On a real-time basis, the aggregates were filmed at an interval of 30 s/frame, using a Nikon CCD camera and documented with NIS-Elements D software (Nikon, Japan). For visualizing cAMP optical density waves, image pairs were subtracted [92] using Image J (NIH, Bethesda, MD).

Under agarose cAMP chemotaxis assay

The under agarose cAMP chemotaxis assay was performed as described previously [128]. Briefly, 100 µl of cell suspension starved at a density of $1x10^7$ cells/ml in KK$_2$ buffer was added to outer troughs and 10 µM cAMP was added in the middle trough of a 1% agarose plate. Cells migrating towards cAMP was recorded every 30 s for 15 min with an inverted Nikon Eclipse TE2000 microscope using NIS-Elements D software (Nikon, Japan). For calculating the average velocity, directionality and chemotactic index, each time 36 cells were analyzed. The cells were tracked using ImageJ. Velocity was calculated by dividing the total displacement of cells by time. Directionality was calculated as the ratio of absolute distance traveled to the total path length, where a maximum value of 1 represents a straight path without deviations. Chemotactic index was calculated as the ratio of the average velocity of a cell moving against a cAMP gradient to the average cell speed. It is a global measure of direction of cell motion.

Quantitative real-time PCR (qRT-PCR)

Total RNA was isolated from AX2 and *tert* KO cells at the indicated time points (0–24 h) using TRIzol reagent (Life Technologies, USA) [129]. RNA samples were quantified with a spectrophotometer (Eppendorf) and were also analyzed on 1% TAE agarose gels. cDNA was synthesized from total RNA using cDNA synthesis kit (Verso, Thermo-scientific). 1 µg of total RNA was used as a template to synthesize cDNA using random primers provided by the manufacturer. 1 µl of cDNA was used for qRT-PCR, using SYBR Green Master Mix (Thermo-scientific). qRT-PCR was carried out to analyze the expression levels of *tert*, *acaA*, *carA*, *pdsA*, *regA*, *pde4*, 5'NT, *countin* and *smlA* using the QuantStudio Flex 7 (Thermo-Fischer). *rnlA* was used as mRNA amplification control. All the qRT-PCR data were analyzed as described [130]. The primer sequences are mentioned in S5 Table.

cAMP quantification

cAMP levels were quantitated using cAMP-XP assay kit as per the manufacturer's protocol (Cell Signalling, USA). AX2 and *tert* KO cells developed on 1% KK$_2$ agar, were lysed with 100 µl of 1X lysis buffer and incubated on ice for 10 min. 50 µl of the lysate and 50 µl HRP-linked cAMP solution were added to the assay plates, incubated at room temperature (RT) on a horizontal orbital shaker. The wells were emptied after 3 h, washed thrice with 200 µl of 1X wash buffer. 100 µl of tetramethylbenzidine (TMB) substrate was added and incubated at RT for 10 min. The reaction was terminated by adding 100 µl of stop solution and the absorbance

was measured at an optical density of 450 nm. The cAMP standard curve was used to calculate absolute cAMP levels.

Glucose quantification

Glucose levels were quantified as per the manufacturer's protocol (GAHK20; Sigma-Aldrich). Mid-log phase cells were harvested and resuspended at a density of 8×10^6 cells/ml in KK$_2$ buffer and kept in shaking conditions at 22˚C. Cells were collected again and lysed by freeze-thaw method. 35 µl of the supernatant was mixed with 200 µl of glucose assay reagent and incubated for 15 min. The absorbance was measured at an optical density of 540 nm. The glucose standard curve was used to calculate absolute glucose levels.

Adenosine quantification

Adenosine quantification was performed as per the manufacturer's protocol (MET5090; Cell-bio Labs). Cells grown in HL5 media were washed and seeded at a density of 5×10^5 cells/cm^2 on KK$_2$ agar plates. The aggregates were harvested using the lysis buffer (62.5 mM Tris-HCl, pH 6.8, 2% SDS, 10% glycerol). 50 µl sample was mixed with control mix (without adenosine deaminase) or reaction mix (with adenosine deaminase) in separate wells and incubated for 15 min. The fluorescence was measured using a spectrofluorometer (Ex- 550 nm, Em- 595 nm). The adenosine fluorescence in the sample was calculated by subtracting fluorescence of control mixed sample from reaction mixed sample. The adenosine standard curve was used to calculate absolute adenosine levels.

Polyphosphate measurements

The conditioned media was incubated with 25 µg/ml DAPI for 5 min and polyphosphate specific fluorescence was measured using a spectrofluorometer (Ex- 415 nm, Em- 550 nm) as previously described [131]. Conditioned medium samples were prepared in FM minimal media to reduce the amount of background fluorescence. Polyphosphate concentration, in terms of phosphate monomers were determined using polyphosphate standards.

ICP-OES

ICP-OES was performed as described previously [99]. Cells were developed on KK$_2$ agar, washed five times in Sorensen phosphate buffer and pelleted. Then, 1 ml of concentrated HNO$_3$ (70%) was added to each sample, and these were further digested by microwave heating. After digestion, the volume of each sample was brought to 9 ml with ultrapure water, filtered with 0.45 mm filter and analysed by ICP-OES (Perkin Elmer Optima 5300 DV ICP-OES). Sample digestion and metal quantification were carried out at the SAIF facility (Sophisticated Analytical Instrument Facility, IIT Madras).

Microscopy

A Nikon SMZ-1000 stereo zoom microscope with epifluorescence optics, Nikon 80i Eclipse upright microscope or a Nikon Eclipse TE2000 inverted microscope equipped with a digital sight DS-5MC camera (Nikon) were used for microscopy. Images were processed with NIS-Elements D (Nikon) or Image J.

Statistical tools

Microsoft Excel (2016) was used for data analyses. Unpaired Student's t-test and two-way ANOVA (GraphPad Prism, version 6) were used to determine the statistical significance.

Supporting information

S1 Fig. Schematic representation of the different functional domains of TERT identified with SMART analysis. TERT protein contains the following domains: a reverse transcriptase (RVT) and an RNA binding domain (Telomerase_RBD).
(TIF)

S2 Fig. Phylogenetic tree showing the relation between *D. discoideum* TERT and TERT from other organisms. Neighbour-Joining Tree was constructed using Muscle alignment of MEGAX (Molecular Evolutionary Genetic Analysis X).
(TIF)

S3 Fig. The tertiary structures of *D. discoideum* and *Tribolium castaneum* TERT. (A) *Tribolium castaneum* TERT. (B) *D. discoideum* TERT. The TERTs of *Tribolium castaneum* (which was used as a template for prediction) and *D. discoideum* have many structural similarities.
(TIF)

S4 Fig. Telomerase activity assay. TRAP assay were performed for AX2 and *tert* KO. Human cell lines HEK and HeLa were used as positive controls. NC is an abbreviation for 'No-Template' control. TrackIT Ultra low range DNA ladder was used.
(TIF)

S5 Fig. Changing cell density and its effect on development. Development assay at different cell density ($2x10^4$ cells/cm^2 to $2x10^6$ cells/cm^2). AX2 cells aggregate even at a cell density below $2x10^4$ cells/cm^2, but *tert* KO fails to aggregate at such a density. *Tert* KO phenotype was not rescued even at higher cell density ($2x10^6$ cells/cm^2).
(TIF)

S6 Fig. Overexpression of hTERT in *tert* KO cells did not rescue the developmental defects.
(TIF)

S7 Fig. Development of other Dictyostelid species in the presence of *tert* KO conditioned medium. *tert* KO-CM did not alter the group size of other dictyostelids. Scale bar: 0.5 mm; (n = 3).
(TIF)

S8 Fig. Cells were starved and developed on KK$_2$ agar plates with AprA and CfaD antibodies (1:300 dilution). Scale bar: 0.5 mm; (n = 3).
(TIF)

S9 Fig. Bright field images of aggregates used for dark field wave optics in [Fig 8].
(TIF)

S10 Fig. Effect of adenosine on aggregate size in *D. discoideum*. A) qRT-PCR of 5'NT during stream breaking. Fold change in mRNA expression is relative to AX2 at the indicated time points. rnlA is used as mRNA amplification control. B) Quantification of adenosine levels during stream breaking. Level of significance is indicated as $^*p{<}0.05$, $^{**}p{<}0.01$, $^{***}p{<}0.001$, and $^{****}p{<}0.0001$.
(TIF)

S11 Fig. Quantification of iron. Iron levels were quantified by ICP-MS. Level of significance is indicated as $^*p{<}0.05$, $^{**}p{<}0.01$, $^{***}p{<}0.001$, and $^{****}p{<}0.0001$.
(TIF)

S12 Fig. Disruption of *tert* affects cell substratum adhesion. Cells were plated at a density of 1×10^5 cells/ml, grown overnight, in an orbital shaker. Floating and attached cells were counted and percentage adhesion was plotted versus rotation speed; (n = 3). Both AX2 and *tert* KO exhibited a sheer force-dependent decrease in substratum adhesion and *tert* KO exhibited significantly reduced adhesion compared to AX2 cells.
(TIF)

S13 Fig. Targeted disruption of *tert* gene (DDB_G0293918) by homologous recombination. A) Physical map of *tert* gene in the genome. PCR primers are shown at positions where they bind. B) The targeting vector (pLPBLP) with sites of recombination and Blasticidin S resistance gene (Bsr). C) Physical map of the genome after targeted gene disruption. D) PCR amplification of DNA using primers that prime outside the vector (P1 FP) and inside the Bsr cassette (BSR RP); no amplicons were obtained from AX2. E) Amplification of the sequence immediately upstream of the *tert* gene (P1 FP) and within the *tert* gene (P2 RP), DNA amplification was observed only in AX2 and not in the *tert* KO clones. F) PCR of genomic sequences flanking the insertion site. A 3.8 kb fragment from AX2 and 1.5 kb amplicon from the *tert* KO were observed. G) RT-PCR of *tert* in the *tert* KO clone. Ig7 (rnlA) was used as an mRNA amplification control.
(TIF)

S1 Table. Protein sequence identity of *Dictyostelium* TERT to other species.
(DOCX)

S2 Table. Primers used for *TRAP* assay.
(DOCX)

S3 Table. Primers used for *tert* KO creation and preliminary genomic DNA PCR screening of *tert* KO cells.
(DOCX)

S4 Table. Primers used for TERT overexpression vector construction.
(DOCX)

S5 Table. Primers used for real-time PCR.
(DOCX)

S1 Video. Timelapse video of AX2 development.
(MP4)

S2 Video. Timelapse video of *tert* KO development.
(MP4)

S3 Video. Timelapse video of *tert* KO (act15/gfp::*tert*) development.
(MP4)

S4 Video. Timelapse video of cAMP wave propagation in AX2.
(MP4)

S5 Video. Timelapse video of cAMP wave propagation in *tert* KO.
(MP4)

Acknowledgments

Author Contributions

Conceptualization: Nasna Nassir, Ramamurthy Baskar.

Data curation: Nasna Nassir, Ramamurthy Baskar.

Formal analysis: Nasna Nassir, Geoffrey J. Hyde, Ramamurthy Baskar.

Funding acquisition: Ramamurthy Baskar.

Investigation: Nasna Nassir.

Methodology: Nasna Nassir, Ramamurthy Baskar.

Project administration: Nasna Nassir, Ramamurthy Baskar.

Resources: Nasna Nassir, Geoffrey J. Hyde, Ramamurthy Baskar.

Software: Nasna Nassir.

Supervision: Ramamurthy Baskar.

Validation: Nasna Nassir.

Visualization: Nasna Nassir, Geoffrey J. Hyde, Ramamurthy Baskar.

Writing – original draft: Nasna Nassir.

Writing – review & editing: Nasna Nassir, Geoffrey J. Hyde, Ramamurthy Baskar.

References

1. Blackburn EH. Telomeres and telomerase: their mechanisms of action and the effects of altering their functions. FEBS letters. 2005; 579(4):859–62. https://doi.org/10.1016/j.febslet.2004.11.036 PMID: 15680963

2. Blackburn EH, Gall JG. A tandemly repeated sequence at the termini of the extrachromosomal ribosomal RNA genes in Tetrahymena. Journal of Molecular Biology. 1978; 120(1):33–53. PMID: 642006

3. Greider CW, Blackburn EH. Identification of a specific telomere terminal transferase activity in tetrahymena extracts. Cell. 1985; 43(2):405–13.

4. Weinrich SL, Pruzan R, Ma L, Ouellette M, Tesmer VM, Holt SE, et al. Reconstitution of human telomerase with the template RNA component hTR and the catalytic protein subunit hTRT. Nature Genetics. 1997; 17(4):498–502. https://doi.org/10.1038/ng1297-498 PMID: 9398860

5. Artandi SE, Chang S, Lee S-L, Alson S, Gottlieb GJ, Chin L, et al. Telomere dysfunction promotes non-reciprocal translocations and epithelial cancers in mice. Nature. 2000; 406(6796):641–5. https://doi.org/10.1038/35020592 PMID: 10949306

6. Aubert G, Lansdorp PM. Telomeres and aging. Physiological reviews. 2008; 88(2):557–79. https://doi.org/10.1152/physrev.00026.2007 PMID: 18391173

7. Keefe DL, Franco S, Liu L, Trimarchi J, Cao B, Weitzen S, et al. Telomere length predicts embryo fragmentation after in vitro fertilization in women—Toward a telomere theory of reproductive aging in women. American Journal of Obstetrics and Gynecology. 2005; 192(4):1256–60. https://doi.org/10.1016/j.ajog.2005.01.036 PMID: 15846215

8. Mu J, Wei LX. Telomere and telomerase in oncology. Cell research. 2002; 12(1):1–7. https://doi.org/10.1038/sj.cr.7290104 PMID: 11942406

9. Parkinson EK, Fitchett C, Cereser B. Dissecting the non-canonical functions of telomerase. Cytogenetic and Genome Research. 2008; 122(3–4):273–80. https://doi.org/10.1159/000167813 PMID: 19188696

10. Teichroeb JH, Kim J, Betts DH. The role of telomeres and telomerase reverse transcriptase isoforms in pluripotency induction and maintenance. RNA Biology. 2016; 13(8):707–19. https://doi.org/10.1080/15476286.2015.1134413 PMID: 26786236

11. Klapper W, Shin T, Mattson MP. Differential regulation of telomerase activity and TERT expression during brain development in mice. Journal of neuroscience research. 2001; 64(3):252–60. https://doi.org/10.1002/jnr.1073 PMID: 11319769

12. Maida Y, Yasukawa M, Furuuchi M, Lassmann T, Possemato R, Okamoto N, et al. An RNA-dependent RNA polymerase formed by TERT and the RMRP RNA. Nature. 2009; 461(7261):230–5. https://doi.org/10.1038/nature08283 PMID: 19701182

13. Ahmed S, Passos JF, Birket MJ, Beckmann T, Brings S, Peters H, et al. Telomerase does not counteract telomere shortening but protects mitochondrial function under oxidative stress. Journal of cell science. 2008; 121(Pt 7):1046–53. https://doi.org/10.1242/jcs.019372 PMID: 18334557

14. Choi J, Southworth LK, Sarin KY, Venteicher AS, Ma W, Chang W, et al. TERT promotes epithelial proliferation through transcriptional control of a Myc- and Wnt-related developmental program. PLoS genetics. 2008; 4(1):e10. https://doi.org/10.1371/journal.pgen.0040010 PMID: 18208333

15. Romaniuk A, Paszel-Jaworska A, Toton E, Lisiak N, Holysz H, Krolak A, et al. The non-canonical functions of telomerase: to turn off or not to turn off. Molecular biology reports. 2019; 46(1):1401–11. https://doi.org/10.1007/s11033-018-4496-x PMID: 30448892

16. Liu Z, Li Q, Li K, Chen L, Li W, Hou M, et al. Telomerase reverse transcriptase promotes epithelial–mesenchymal transition and stem cell-like traits in cancer cells. Oncogene. 2013; 32(36):4203. https://doi.org/10.1038/onc.2012.441 PMID: 23045275

17. Gilson E, Ségal-Bendirdjian E. The telomere story or the triumph of an open-minded research. Biochimie. 2010; 92(4):321–6. https://doi.org/10.1016/j.biochi.2009.12.014 PMID: 20096746

18. McClintock B. The Behavior in Successive Nuclear Divisions of a Chromosome Broken at Meiosis. PNAS. 1939; 25(8):405–16. https://doi.org/10.1073/pnas.25.8.405 PMID: 16577924

19. McClintock B. The stability of broken ends of chromosomes in Zea mays. Genetics. 1941; 26(2):234. PMID: 17247004

20. Muller HJ. The remaking of chromosomes. Collecting net. 1938; 13:181–98.

21. Szostak JW, Blackburn EH. Cloning yeast telomeres on linear plasmid vectors. Cell. 1982; 29(1):245–55. PMID: 6286143

22. Annesley SJ, Fisher PR. Dictyostelium discoideum—a model for many reasons. Molecular and cellular biochemistry. 2009; 329(1–2):73–91. https://doi.org/10.1007/s11010-009-0111-8 PMID: 19387798

23. Maniak M. Dictyostelium as a model for human lysosomal and trafficking diseases. Seminars in Cell and Developmental Biology. 2011; 22(1):114–9. https://doi.org/10.1016/j.semcdb.2010.11.001 PMID: 21056680

24. Muller-Taubenberger A, Kortholt A, Eichinger L. Simple system—substantial share: the use of Dictyostelium in cell biology and molecular medicine. European journal of cell biology. 2013; 92(2):45–53. https://doi.org/10.1016/j.ejcb.2012.10.003 PMID: 23200106

25. Williams JG. Dictyostelium Finds New Roles to Model. Genetics. 2010; 185(3):717–26. https://doi.org/10.1534/genetics.110.119297 PMID: 20660652

26. Williams RSB, Boeckeler K, Gräf R, Müller-Taubenberger A, Li Z, Isberg RR, et al. Towards a molecular understanding of human diseases using Dictyostelium discoideum. Trends in Molecular Medicine. 2006; 12(9):415–24. https://doi.org/10.1016/j.molmed.2006.07.003 PMID: 16890490

27. Hohl HR, Raper KB. Control of sorocarp size in the cellular slime mold Dictyostelium discoideum. Developmental biology. 1964; 9(1):137–53.

28. Brock DA, Buczynski G, Spann TP, Wood SA, Cardelli J, Gomer RH. A Dictystelium mutant with defective aggregate size determination. Development. 1996; 122(9):2569–78. PMID: 8787732

29. Brock DA, Ehrenman K, Ammann R, Tang Y, Gomer RH. Two components of a secreted cell number-counting factor bind to cells and have opposing effects on cAMP signal transduction in Dictyostelium. The Journal of biological chemistry. 2003; 278(52):52262–72. https://doi.org/10.1074/jbc.M309101200 PMID: 14557265

30. Brock DA, Gomer RH. A cell-counting factor regulating structure size in Dictyostelium. Genes & development. 1999; 13(15):1960–9.

31. Brock DA, Gomer RH. A secreted factor represses cell proliferation in Dictyostelium. Development. 2005; 132(20):4553–62. https://doi.org/10.1242/dev.02032 PMID: 16176950

32. Brown JM, Firtel RA. Just the right size: cell counting in Dictyostelium. Trends in genetics: TIG. 2000; 16(5):191–3. PMID: 10782107

33. Gomer RH, Jang W, Brazill D. Cell density sensing and size determination. Development, growth & differentiation. 2011; 53(4):482–94.

34. Jain R, Yuen IS, Taphouse CR, Gomer RH. A density-sensing factor controls development in Dictyostelium. Genes and development. 1992; 6(3):390–400. https://doi.org/10.1101/gad.6.3.390 PMID: 1547939

35. Jaiswal P, Soldati T, Thewes S, Baskar R. Regulation of aggregate size and pattern by adenosine and caffeine in cellular slime molds. BMC developmental biology. 2012; 12:5. https://doi.org/10.1186/1471-213X-12-5 PMID: 22269093

36. Mehdy MC, Firtel RA. A secreted factor and cyclic AMP jointly regulate cell-type-specific gene expression in Dictyostelium discoideum. Molecular and Cellular Biology. 1985; 5(4):705–13. https://doi.org/10.1128/mcb.5.4.705 PMID: 2985966

37. Brock DA, Hatton RD, Giurgiutiu DV, Scott B, Ammann R, Gomer RH. The different components of a multisubunit cell number-counting factor have both unique and overlapping functions. Development. 2002; 129(15):3657–68. PMID: 12117815

38. Brock DA, Hatton RD, Giurgiutiu DV, Scott B, Jang W, Ammann R, et al. CF45-1, a secreted protein which participates in Dictyostelium group size regulation. Eukaryotic cell. 2003; 2(4):788–97. https://doi.org/10.1128/EC.2.4.788-797.2003 PMID: 12912898

39. Bonner JT, Hoffman ME. Evidence for a Substance Responsible for the Spacing Pattern of Aggregation and Fruiting in the Cellular Slime Molds. Journal of Embryology and Experimental Morphology. 1963; 11(3):571.

40. Loomis W. Dictyostelium discoideum: a developmental system. Cell. 2012. Elsevier.

41. Roisin-Bouffay C, Jang W, Caprette DR, Gomer RH. A precise group size in Dictyostelium is generated by a cell-counting factor modulating cell-cell adhesion. Molecular cell. 2000; 6(4):953–9. PMID: 11090633

42. Bakthavatsalam D, Brock DA, Nikravan NN, Houston KD, Hatton RD, Gomer RH. The secreted Dictyostelium protein CfaD is a chalone. Journal of cell science. 2008; 121(Pt 15):2473–80. https://doi.org/10.1242/jcs.026682 PMID: 18611962

43. Suess PM, Watson J, Chen W, Gomer RH. Extracellular polyphosphate signals through Ras and Akt to prime Dictyostelium discoideum cells for development. Journal of cell science. 2017; 130(14):2394–404. https://doi.org/10.1242/jcs.203372 PMID: 28584190

44. Mayanagi T, Amagai A, Maeda Y. DNG1, a Dictyostelium homologue of tumor suppressor ING1 regulates differentiation of Dictyostelium cells. Cellular and molecular life sciences: CMLS. 2005; 62 (15):1734–43. https://doi.org/10.1007/s00018-005-4570-0 PMID: 16003496

45. Sasaki K, Chae SC, Loomis WF, Iranfar N, Amagai A, Maeda Y. An immediate-early gene, srsA: its involvement in the starvation response that initiates differentiation of Dictyostelium cells. Differentiation. 2008; 76(10):1093–103. https://doi.org/10.1111/j.1432-0436.2008.00298.x PMID: 18673382

46. Bolourani P, Spiegelman GB, Weeks G. Delineation of the roles played by RasG and RasC in cAMP-dependent signal transduction during the early development of Dictyostelium discoideum. Molecular biology of the cell. 2006; 17(10):4543–50. https://doi.org/10.1091/mbc.E05-11-1019 PMID: 16885420

47. Van Haastert PJ, Kien E. Binding of cAMP derivatives to Dictyostelium discoideum cells. Activation mechanism of the cell surface cAMP receptor. The Journal of biological chemistry. 1983; 258 (16):9636–42. PMID: 6309778

48. Van Haastert PJ. Sensory adaptation of Dictyostelium discoideum cells to chemotactic signals. The Journal of cell biology. 1983; 96(6):1559–65. https://doi.org/10.1083/jcb.96.6.1559 PMID: 6304109

49. Chisholm RL, Firtel RA. Insights into morphogenesis from a simple developmental system. Nature reviews Molecular cell biology. 2004; 5(7):531–41. https://doi.org/10.1038/nrm1427 PMID: 15232571

50. Wang B, Kuspa A. Dictyostelium development in the absence of cAMP. Science. 1997; 277 (5323):251–4. PMID: 9211856

51. Rutherford CL, Overall DF, Ubeidat M, Joyce BR. Analysis of 5' nucleotidase and alkaline phosphatase by gene disruption in Dictyostelium. Genesis. 2003; 35(4):202–13. https://doi.org/10.1002/gene.10185 PMID: 12717731

52. Garcia GL, Rericha EC, Heger CD, Goldsmith PK, Parent CA. The group migration of Dictyostelium cells is regulated by extracellular chemoattractant degradation. Molecular biology of the cell. 2009; 20 (14):3295–304. https://doi.org/10.1091/mbc.E09-03-0223 PMID: 19477920

53. Bader S, Kortholt A, Snippe H, Van Haastert PJ. DdPDE4, a novel cAMP-specific phosphodiesterase at the surface of dictyostelium cells. The Journal of biological chemistry. 2006; 281(29):20018–26. https://doi.org/10.1074/jbc.M600040200 PMID: 16644729

54. Gomer RH, Yuen IS, Firtel RA. A secreted 80 × 10(3) Mr protein mediates sensing of cell density and the onset of development in Dictyostelium. Development. 1991; 112(1):269. PMID: 1663029

55. Loomis WF. Cell signaling during development of Dictyostelium. Developmental Biology. 2014; 391 (1):1–16. https://doi.org/10.1016/j.ydbio.2014.04.001 PMID: 24726820

56. Ma H, Gamper M, Parent C, Firtel RA. The Dictyostelium MAP kinase kinase DdMEK1 regulates chemotaxis and is essential for chemoattractant-mediated activation of guanylyl cyclase. The EMBO journal. 1997; 16(14):4317–32. https://doi.org/10.1093/emboj/16.14.4317 PMID: 9250676

57. Schaap P, Wang M. Interactions between adenosine and oscillatory cAMP signaling regulate size and pattern in Dictyostelium. Cell. 1986; 45(1):137–44. PMID: 3006924

58. Fey P, Stephens S, Titus MA, Chisholm RL. SadA, a novel adhesion receptor in Dictyostelium. The Journal of cell biology. 2002; 159(6):1109–19. https://doi.org/10.1083/jcb.200206067 PMID: 12499361

59. Gao T, Knecht D, Tang L, Hatton RD, Gomer RH. A cell number counting factor regulates Akt/protein kinase B to regulate Dictyostelium discoideum group size. Eukaryotic cell. 2004; 3(5):1176–84. https://doi.org/10.1128/EC.3.5.1176-1184.2004 PMID: 15470246

60. Swaney KF, Huang CH, Devreotes PN. Eukaryotic chemotaxis: a network of signaling pathways controls motility, directional sensing, and polarity. Annual review of biophysics. 2010; 39:265–89. https://doi.org/10.1146/annurev.biophys.093008.131228 PMID: 20192768

61. Varnum B, Soll DR. Effects of cAMP on single cell motility in Dictyostelium. The Journal of cell biology. 1984; 99(3):1151–5. https://doi.org/10.1083/jcb.99.3.1151 PMID: 6088555

62. Jang W, Gomer RH. Exposure of cells to a cell number-counting factor decreases the activity of glucose-6-phosphatase to decrease intracellular glucose levels in Dictyostelium discoideum. Eukaryotic cell. 2005; 4(1):72–81. https://doi.org/10.1128/EC.4.1.72-81.2005 PMID: 15643062

63. Jang W, Gomer RH. A protein in crude cytosol regulates glucose-6-phosphatase activity in crude microsomes to regulate group size in Dictyostelium. The Journal of biological chemistry. 2006; 281 (24):16377–83. https://doi.org/10.1074/jbc.M509995200 PMID: 16606621

64. Jang W, Chiem B, Gomer RH. A secreted cell number counting factor represses intracellular glucose levels to regulate group size in dictyostelium. The Journal of biological chemistry. 2002; 277 (42):39202–8. https://doi.org/10.1074/jbc.M205635200 PMID: 12161440

65. Tang L, Gao T, McCollum C, Jang W, Vicker MG, Ammann RR, et al. A cell number-counting factor regulates the cytoskeleton and cell motility in Dictyostelium. Proceedings of the National Academy of Sciences of the United States of America. 2002; 99(3):1371–6. https://doi.org/10.1073/pnas.022516099 PMID: 11818526

66. Varnum B, Edwards KB, Soll DR. The developmental regulation of single-cell motility in Dictyostelium discoideum. Dev Biol. 1986; 113(1):218–27. PMID: 3943662

67. Coates JC, Harwood AJ. Cell-cell adhesion and signal transduction during Dictyostelium development. Journal of cell science. 2001; 114(Pt 24):4349–58. PMID: 11792801

68. Tang L, Ammann R, Gao T, Gomer RH. A cell number-counting factor regulates group size in Dictyostelium by differentially modulating cAMP-induced cAMP and cGMP pulse sizes. The Journal of biological chemistry. 2001; 276(29):27663–9. https://doi.org/10.1074/jbc.M102205200 PMID: 11371560

69. Beug H, Katz FE, Gerisch G. Dynamics of antigenic membrane sites relating to cell aggregation in Dictyostelium discoideum. The Journal of cell biology. 1973; 56(3):647–58. https://doi.org/10.1083/jcb.56.3.647 PMID: 4631665

70. Yang C, Brar SK, Desbarats L, Siu CH. Synthesis of the Ca(2+)-dependent cell adhesion molecule DdCAD-1 is regulated by multiple factors during Dictyostelium development. Differentiation; research in biological diversity. 1997; 61(5):275–84. https://doi.org/10.1046/j.1432-0436.1997.6150275.x PMID: 9342838

71. Tarantola M, Bae A, Fuller D, Bodenschatz E, Loomis W. Cell Substratum Adhesion during Early Development of Dictyostelium discoideum. PLoS One. 2014; 9(9):e106574. https://doi.org/10.1371/journal.pone.0106574 PMID: 25247557

72. Iversen OH. Some theoretical considerations on chalones and the treatment of cancer: a review. Cancer research. 1970; 30(5):1481–4. PMID: 4248282

73. Gaudet P, Fey P, Basu S, Bushmanova YA, Dodson R, Sheppard KA, et al. dictyBase update 2011: web 2.0 functionality and the initial steps towards a genome portal for the AmoebozoDDB0192195. Nucleic acids research. 2011; 39(Database issue):D620–4. https://doi.org/10.1093/nar/gkq1103 PMID: 21087999

74. Eichinger L, Pachebat JA, Glockner G, Rajandream MA, Sucgang R, Berriman M, et al. The genome of the social amoeba Dictyostelium discoideum. Nature. 2005; 435(7038):43–57. https://doi.org/10.1038/nature03481 PMID: 15875012

75. Sýkorová E, Fajkus J. Structure-function relationships in telomerase genes. Biology of the cell. 2009; 101(7):375–406. https://doi.org/10.1042/BC20080205 PMID: 19419346

76. Cong YS, Wright WE, Shay JW. Human telomerase and its regulation. Microbiology and molecular biology reviews: MMBR. 2002; 66(3):407–25. https://doi.org/10.1128/MMBR.66.3.407-425.2002 PMID: 12208997

77. Kumar S, Stecher G, Li M, Knyaz C, Tamura K. MEGA X: Molecular Evolutionary Genetics Analysis across Computing Platforms. Molecular biology and evolution. 2018; 35(6):1547–9. https://doi.org/10.1093/molbev/msy096 PMID: 29722887

78. Saitou N, Nei M. The neighbor-joining method: a new method for reconstructing phylogenetic trees. Molecular biology and evolution. 1987; 4(4):406–25. https://doi.org/10.1093/oxfordjournals.molbev.a040454 PMID: 3447015

79. Lin J, Epel E, Cheon J, Kroenke C, Sinclair E, Bigos M, et al. Analyses and comparisons of telomerase activity and telomere length in human T and B cells: insights for epidemiology of telomere maintenance. Journal of immunological methods. 2010; 352(1–2):71–80. https://doi.org/10.1016/j.jim.2009.09.012 PMID: 19837074

80. Gan Y, Lu J, Johnson A, Wientjes MG, Schuller DE, Au JL. A quantitative assay of telomerase activity. Pharmaceutical research. 2001; 18(4):488–93. PMID: 11451036

81. Fitzgerald MS, McKnight TD, Shippen DE. Characterization and developmental patterns of telomerase expression in plants. Proceedings of the National Academy of Sciences of the United States of America. 1996; 93(25):14422–7. https://doi.org/10.1073/pnas.93.25.14422 PMID: 8962067

82. Tan TC, Rahman R, Jaber-Hijazi F, Felix DA, Chen C, Louis EJ, et al. Telomere maintenance and telomerase activity are differentially regulated in asexual and sexual worms. Proceedings of the National Academy of Sciences of the United States of America. 2012; 109(11):4209–14. https://doi.org/10.1073/pnas.1118885109 PMID: 22371573

83. Lin JJ, Zakian VA. An in vitro assay for Saccharomyces telomerase requires EST1. Cell. 1995; 81 (7):1127–35. PMID: 7600580

84. Schumpert C, Nelson J, Kim E, Dudycha JL, Patel RC. Telomerase activity and telomere length in Daphnia. PloS one. 2015; 10(5):e0127196. https://doi.org/10.1371/journal.pone.0127196 PMID: 25962144

85. Eichinger L, Noegel AA. Comparative genomics of Dictyostelium discoideum and Entamoeba histolytica. Current opinion in microbiology. 2005; 8(5):606–11. https://doi.org/10.1016/j.mib.2005.08.009 PMID: 16125444

86. Shay JW, Zou Y, Hiyama E, Wright WE. Telomerase and cancer. Human molecular genetics. 2001; 10(7):677–85. https://doi.org/10.1093/hmg/10.7.677 PMID: 11257099

87. Cristofari G, Lingner J. Telomere length homeostasis requires that telomerase levels are limiting. The EMBO journal. 2006; 25(3):565–74. https://doi.org/10.1038/sj.emboj.7600952 PMID: 16424902

88. Riedel V, Gerisch G, Muller E, Beug H. Defective cyclic adenosine-3', 5'-phosphate-phosphodiesterase regulation in morphogenetic mutants of Dictyostelium discoideum. Journal of molecular biology. 1973; 74(4):573–85. PMID: 4354075

89. Faure M, Podgorski GJ, Franke J, Kessin RH. Disruption of Dictyostelium discoideum morphogenesis by overproduction of cAMP phosphodiesterase. Proceedings of the National Academy of Sciences of the United States of America. 1988; 85(21):8076–80. https://doi.org/10.1073/pnas.85.21.8076 PMID: 2847151

90. Kesbeke F, Van Haastert PJ. Reduced cAMP secretion in Dictyostelium discoideum mutant HB3. Developmental biology. 1988; 130(2):464–70. PMID: 2848740

91. Weijer CJ. Dictyostelium morphogenesis. Current opinion in genetics & development. 2004; 14 (4):392–8.

92. Siegert F, Weijer CJ. Spiral and concentric waves organize multicellular Dictyostelium mounds. Current biology: CB. 1995; 5(8):937–43. PMID: 7583152

93. El-Brolosy MA, Stainier DYR. Genetic compensation: A phenomenon in search of mechanisms. PLOS Genetics. 2017; 13(7):e1006780. https://doi.org/10.1371/journal.pgen.1006780 PMID: 28704371

94. Tautz D. Problems and paradigms: Redundancies, development and the flow of information. BioEssays. 1992; 14(4):263–6. https://doi.org/10.1002/bies.950140410 PMID: 1596275

95. Darmon M, Brachet P, Da Silva LH. Chemotactic signals induce cell differentiation in Dictyostelium discoideum. Proceedings of the National Academy of Sciences of the United States of America. 1975; 72 (8):3163–6. https://doi.org/10.1073/pnas.72.8.3163 PMID: 171655

96.   Mann SK, Firtel RA. Cyclic AMP regulation of early gene expression in Dictyostelium discoideum: mediation via the cell surface cyclic AMP receptor. Molecular and cellular biology. 1987; 7(1):458–69. https://doi.org/10.1128/mcb.7.1.458 PMID: 3031475

97.   Theibert A, Devreotes PN. Adenosine and its derivatives inhibit the cAMP signaling response in Dictyostelium discoideum. Developmental biology. 1984; 106(1):166–73. PMID: 6092178

98.   Brenner M, Thoms SD. Caffeine blocks activation of cyclic AMP synthesis in Dictyostelium discoideum. Developmental biology. 1984; 101(1):136–46. PMID: 6319207

99.   Buracco S, Peracino B, Andreini C, Bracco E, Bozzaro S. Differential Effects of Iron, Zinc, and Copper on Dictyostelium discoideum Cell Growth and Resistance to Legionella pneumophila. Frontiers in cellular and infection microbiology. 2017; 7:536. https://doi.org/10.3389/fcimb.2017.00536 PMID: 29379774

100.   Bachand F, Autexier C. Functional regions of human telomerase reverse transcriptase and human telomerase RNA required for telomerase activity and RNA-protein interactions. Molecular and cellular biology. 2001; 21(5):1888–97. https://doi.org/10.1128/MCB.21.5.1888-1897.2001 PMID: 11238925

101.   Lue NF, Lin YC, Mian IS. A conserved telomerase motif within the catalytic domain of telomerase reverse transcriptase is specifically required for repeat addition processivity. Molecular and cellular biology. 2003; 23(23):8440–9. https://doi.org/10.1128/MCB.23.23.8440-8449.2003 PMID: 14612390

102.   Wyatt HD, Tsang AR, Lobb DA, Beattie TL. Human telomerase reverse transcriptase (hTERT) Q169 is essential for telomerase function in vitro and in vivo. PloS one. 2009; 4(9):e7176. https://doi.org/10.1371/journal.pone.0007176 PMID: 19777057

103.   Hossain S, Singh S, Lue NF. Functional analysis of the C-terminal extension of telomerase reverse transcriptase. A putative "thumb" domain. The Journal of biological chemistry. 2002; 277(39):36174–80. https://doi.org/10.1074/jbc.M201976200 PMID: 12151386

104.   Robart AR, Collins K. Human telomerase domain interactions capture DNA for TEN domain-dependent processive elongation. Molecular cell. 2011; 42(3):308–18. https://doi.org/10.1016/j.molcel.2011.03.012 PMID: 21514196

105.   Heidel AJ, Lawal HM, Felder M, Schilde C, Helps NR, Tunggal B, et al. Phylogeny-wide analysis of social amoeba genomes highlights ancient origins for complex intercellular communication. Genome research. 2011; 21(11):1882–91. https://doi.org/10.1101/gr.121137.111 PMID: 21757610

106.   Fujiwara H, Osanai M, Matsumoto T, Kojima KK. Telomere-specific non-LTR retrotransposons and telomere maintenance in the silkworm, Bombyx mori. Chromosome research: an international journal on the molecular, supramolecular and evolutionary aspects of chromosome biology. 2005; 13(5):455–67.

107.   Tatsuke T, Sakashita K, Masaki Y, Lee JM, Kawaguchi Y, Kusakabe T. The telomere-specific non-LTR retrotransposons SART1 and TRAS1 are suppressed by Piwi subfamily proteins in the silkworm, Bombyx mori. Cellular & molecular biology letters. 2010; 15(1):118–33.

108.   Kubo Y, Okazaki S, Anzai T, Fujiwara H. Structural and phylogenetic analysis of TRAS, telomeric repeat-specific non-LTR retrotransposon families in Lepidopteran insects. Molecular biology and evolution. 2001; 18(5):848–57. https://doi.org/10.1093/oxfordjournals.molbev.a003866 PMID: 11319268

109.   Okazaki S, Ishikawa H, Fujiwara H. Structural analysis of TRAS1, a novel family of telomeric repeat-associated retrotransposons in the silkworm, Bombyx mori. Molecular and cellular biology. 1995; 15 (8):4545–52. https://doi.org/10.1128/mcb.15.8.4545 PMID: 7623845

110.   Traut W, Szczepanowski M, Vitkova M, Opitz C, Marec F, Zrzavy J. The telomere repeat motif of basal Metazoa. Chromosome research. 2007; 15(3):371–82. https://doi.org/10.1007/s10577-007-1132-3 PMID: 17385051

111.   Subramanian L, Moser BA, Nakamura TM. Recombination-based telomere maintenance is dependent on Tel1-MRN and Rap1 and inhibited by telomerase, Taz1, and Ku in fission yeast. Molecular and cellular biology. 2008; 28(5):1443–55. https://doi.org/10.1128/MCB.01614-07 PMID: 18160711

112.   Pardue ML, Rashkova S, Casacuberta E, DeBaryshe PG, George JA, Traverse KL. Two retrotransposons maintain telomeres in Drosophila. Chromosome research. 2005; 13(5):443–53. https://doi.org/10.1007/s10577-005-0993-6 PMID: 16132810

113.   Casacuberta E. Drosophila: Retrotransposons Making up Telomeres. Viruses. 2017; 9(7).

114.   Bürglin TR, Affolter M. Homeodomain proteins: an update. Chromosoma. 2016; 125(3):497–521. https://doi.org/10.1007/s00412-015-0543-8 PMID: 26464018

115.   Gehring WJ, Affolter M, Bürglin T. HOMEODOMAIN PROTEINS. Annual Review of Biochemistry. 1994; 63(1):487–526.

116.   Matsuo T, Shimose S, Kubo T, Fujimori J, Yasunaga Y, Sugita T, et al. Correlation between p38 mitogen-activated protein kinase and human telomerase reverse transcriptase in sarcomas. Journal of experimental & clinical cancer research: CR. 2012; 31:5.

117. Serrano D, Bleau AM, Fernandez-Garcia I, Fernandez-Marcelo T, Iniesta P, Ortiz-de-Solorzano C, et al. Inhibition of telomerase activity preferentially targets aldehyde dehydrogenase-positive cancer stem-like cells in lung cancer. Molecular cancer. 2011; 10:96. https://doi.org/10.1186/1476-4598-10-96 PMID: 21827695

118. Ehrenman K, Yang G, Hong WP, Gao T, Jang W, Brock DA, et al. Disruption of aldehyde reductase increases group size in dictyostelium. The Journal of biological chemistry. 2004; 279(2):837–47. https://doi.org/10.1074/jbc.M310539200 PMID: 14551196

119. Singh SP, Dhakshinamoorthy R, Jaiswal P, Schmidt S, Thewes S, Baskar R. The thyroxine inactivating gene, type III deiodinase, suppresses multiple signaling centers in Dictyostelium discoideum. Developmental biology. 2014; 396(2):256–68. https://doi.org/10.1016/j.ydbio.2014.10.012 PMID: 25446527

120. Mohamed W, Ray S, Brazill D, Baskar R. Absence of catalytic domain in a putative protein kinase C (PkcA) suppresses tip dominance in Dictyostelium discoideum. Developmental biology. 2015; 405 (1):10–20. https://doi.org/10.1016/j.ydbio.2015.05.021 PMID: 26183108

121. Fey P, Kowal AS, Gaudet P, Pilcher KE, Chisholm RL. Protocols for growth and development of Dictyostelium discoideum. Nature protocols. 2007; 2(6):1307–16. https://doi.org/10.1038/nprot.2007.178 PMID: 17545967

122. Damm K, Hemmann U, Garin-Chesa P, Hauel N, Kauffmann I, Priepke H, et al. A highly selective telomerase inhibitor limiting human cancer cell proliferation. The EMBO journal. 2001; 20(24):6958–68. https://doi.org/10.1093/emboj/20.24.6958 PMID: 11742973

123. Seimiya H, Oh-hara T, Suzuki T, Naasani I, Shimazaki T, Tsuchiya K, et al. Telomere shortening and growth inhibition of human cancer cells by novel synthetic telomerase inhibitors MST-312, MST-295, and MST-1991. Molecular cancer therapeutics. 2002; 1(9):657–65. PMID: 12479362

124. Kim NW, Wu F. Advances in quantification and characterization of telomerase activity by the telomeric repeat amplification protocol (TRAP). Nucleic acids research. 1997; 25(13):2595–7. https://doi.org/10.1093/nar/25.13.2595 PMID: 9185569

125. Mender I, Shay JW. Telomerase Repeated Amplification Protocol (TRAP). Bio-protocol. 2015; 5(22).

126. Gomer RH, Yuen IS, Firtel RA. A secreted 80 x 10(3) Mr protein mediates sensing of cell density and the onset of development in Dictyostelium. Development. 1991; 112(1):269–78. PMID: 1663029

127. Desbarats L, Brar SK, Siu CH. Involvement of cell-cell adhesion in the expression of the cell cohesion molecule gp80 in Dictyostelium discoideum. Journal of cell science. 1994; 107 (Pt 6):1705–12.

128. Woznica D, Knecht DA. Under-agarose chemotaxis of Dictyostelium discoideum. Methods in molecular biology. 2006; 346:311–25. https://doi.org/10.1385/1-59745-144-4:311 PMID: 16957299

129. Pilcher KE, Gaudet P, Fey P, Kowal AS, Chisholm RL. A general purpose method for extracting RNA from Dictyostelium cells. Nature protocols. 2007; 2(6):1329–32. https://doi.org/10.1038/nprot.2007.191 PMID: 17545970

130. Schmittgen TD, Livak KJ. Analyzing real-time PCR data by the comparative C(T) method. Nature protocols. 2008; 3(6):1101–8. PMID: 18546601

131. Aschar-Sobbi R, Abramov AY, Diao C, Kargacin ME, Kargacin GJ, French RJ, et al. High sensitivity, quantitative measurements of polyphosphate using a new DAPI-based approach. Journal of fluorescence. 2008; 18(5):859–66. https://doi.org/10.1007/s10895-008-0315-4 PMID: 18210191